JPRS-UEQ-91-003
8 MARCH 1991

Foreign Broadcast Information Service 50 ANNIVERSARY 1941 - 1991

JPRS Report

Science & Technology

USSR: Engineering & Equipment

Science & Technology

USSR: Engineering & Equipment

JPRS-UEQ-91-003 *8 March 1991*

CONTENTS

UDC 621.089.5:621.375.826

Determining Certain Energy Parameters of Laser Radiation on Basis of Frequency and Time Interval Measurements

917F0071C Moscow IZMERITELNAYA TEKHNIKA in Russian No 10, Oct 90 pp 24-26

[Article by B.N. Morozov]

[Abstract] The feasibility of determining the laser radiation power and its distribution over the laser beam cross-section on the basis of frequency and time interval readings is demonstrated, considering that the calorimetric method yields the average power within 1-3% and the self-calibration method is accurate within 0.05-0.1% but is applicable to lasers in the 1 mW power range. While both methods are applicable to continuous-wave, pulsed, and periodically pulsed lasers, so are frequency measurements and these are today the most accurate of all. The proposed method utilizes the optical rectification effect, namely p-polarization of radiation fluctuations or the radiation envelope within some a time interval as the laser beam passes through a nonlinear crystal with known properties. The power laser radiation impinging on an electrooptic crystal between the two plates of a capacitor produces a voltage across those plates of such "crystal capacitor", a voltage differently dependent on the incident power of a continuous-wave laser and on that of a pulsed laser. If now the capacitor is connected to an inductance, they form a tank circuit into which a precision frequency meter can be inserted. The oscillation frequency, as well as the capacitor voltage will depend on the incident laser power, all geometrical and "electrical" parameters in this relation (l- length of crystal, w- width of crystal, C- capacitance of "crystal" capacitor, L- inductance of tank circuit, R- resistance of tank circuit) being accurately measurable. Inasmuch the nonlinear susceptibility of a crystal is the least accurately measured quantity in this system, its measurement error contributes most to the inaccuracy of laser power determination. This error can be eliminated dividing the laser beam into two with, say, a splitter plate for two identical "crystal" capacitors in a separate tank circuit each and measuring the power ratio. Not only is the dielectric susceptibility thus eliminated as a parameter, but also voltage, capacitance, and frequency ratios are more accurate than readings of the respective absolute magnitudes. For measuring the sum power in this case, the two capacitors must be connected in parallel in a common tank circuit. In order to determine the average power of pulsed lasers and especially monopulse lasers, it becomes necessary to measure time intervals as well. Because optical rectification has no threshold, oscillations in the tank circuit will occur already at very low levels of incident laser power. Quantum fluctuations are, moreover, negligible in comparison with the instability of laser radiation. On the basis of all these considerations, a feedthrough laser-power meter has been developed at the All-Union Scientific Research Institute of Engineering Physics and Radio Engineering Measurements which can operate at a laser radiation intensity of the order of 10 GW/cm^2 and is not only suitable for single-frequency lasers but also adaptable for dual-frequency lasers. Figures 2; references 14.

UDC 543.812.08:665.6

Quick-Test Hygrometer for Commercial Crude Oil

917F0071D Moscow IZMERITELNAYA TEKHNIKA in Russian No 10, Oct 90 pp 58-59

[Article by G.G. Glukhov, Yu.S. Maslennikov, V.A. Cha, and V.P. Shiyan]

[Abstract] A hygrometer for measuring the moisture content in commercial crude oil by the resonance method with centimetric waves is described, an experimental prototype having already been built. It consists of a 9.764 GHz Gunn-diode oscillator, a ferrite decoupler, an attenuator, a prismatic cavity resonator with an exciter probe in the entrance window and a pickup probe in the exit window, a teflon sampling tube which passes through the cavity along its axis between the two probes, and a microwave diode detector behind the pickup probe followed by an indicating device such as a voltmeter. While crude oil is pumped through the tube, a signal proportional to the water content is picked up. The detector output voltage is also proportional to the oscillator output power and serves as measure of the water content. Using the frequency shift as measure, a more accurate one, would require addition of a frequency meter and thus complicate the apparatus. A high sensitivity of about 2.17 dB/ % H_2O has been attained by adjusting the length of the cavity for excitation of an H_{103} mode. For water contents within the 1-3% range the relative error of measurements does not exceed 1%. The instrument was tested on mixtures of crude oil not only with water but also with toluene (1.5:1), hexane (1.5:1), and 100 g/l aqueous NaCl solution at room temperature (20°C). The systematic error associated with sample preparation does not exceed 1%. The instrument error reduces to the error of cavity tuning to resonance, which shifts as crude oil begins to flow through the initially empty tube. Considering that the frequency stability of the microwave oscillator is very high, within 10^{-7}, the instrument error is determined by cavity Q-factor under load and by the voltmeter accuracy. The instrument must be calibrated against dry crude oil for each crude oil with a different C:H ratio and from a different deposit. Figures 2; references 2.

UDC 681.2.083:535.321

Experimental Study of Quick Inspection of Optical Fibers on Basis of Index Profile

917F0071B Moscow IZMERITELNAYA TEKHNIKA in Russian No 10, Oct 90 pp 22-24

[Article by A.B. Androsik and S.D. Mirovitskaya]

[Abstract] Inspection of optical fibers by the refraction method is described and analyzed, this method having been studied experimentally with a laser as source of coherent monochromatic radiation needed for index profile measurements. A narrow laser beam was formed by two objectives and a pinhole filter-diaphragm. This beam was passed through a test cell containing immersion fluid with a fiber specimen in it. The overall length of this refractometer was shortened by having two plane mirrors reverse the path of light upon two successive 90° deflections. The beam radiation intensity, varied by means of two polarizers and an a pair of attenuators, was recorded by a CCD (charge-coupled-devices) photodetector array transmitting electric signals to an oscillograph. The components of this inspection instrument were arranged in the following sequence: laser → first objective → first polarizer → first mirror → diaphragm → second mirror → second polarizer → second objective before test cell, followed by third objective → contiguous pair of attenuator plates → photodetector. The laser beam scanned a fiber specimen from the center of the core to the surface of the sheath. The immersion fluid matched the fiber material optically, with an identical refractive index, several fluids having been tested alone without a fiber and the best one selected. This method facilitates detection of geometrical as well as optical defects, the major source of error being lateral and axial displacements of the fiber specimen during inspection. The effect of its displacements on the scattered field in the photodetector and thus on the distortion of the projected fiber image depends essentially on the characteristics of the optical components and on their configuration. The maximum fiber displacement not influencing the scattered field in the photodetector can be calculated on the basis of a geometrical analysis and numerically estimated on the basis of the experimental data. Figures 2; references 3.

UDC 531.717.1.082.5.088.3:681.7.068

Improving Accuracy of Diffraction Method for Measuring Diameter of Thin Homogeneous Optical Fibers

917F0071A Moscow IZMERITELNAYA TEKHNIKA in Russian No 10, Oct 90 pp 20-22

[Article by A.B. Veselvskiy, A.S. Mitrofanov, and V.N. Poyarkov]

[Abstract] The diffraction method of measuring the diameter of thin optical fibers is analyzed for causes of low accuracy, the fiber diameter being one of the parameters along with the wavelength and the refractive index in the relation between the angular dimensions of diffraction fringes and the scattering angle. The fringe dimension is a monotonic function of the scattering angle in geometrical optics and this is adequate for determination of the diameters of thick fibers from the average angular dimension of fringes within some scattering sector. According to the wave theory, however, it is a sinusoidal or sinusoidally modulated rather than monotonic function of the scattering angle and this gives rise to ambiguity in determination of the diameters of thin fibers. Diameters of fibers within the 5-50 μm range can be more accurately determined on the basis of the scattering indicatrix in accordance with the Kerker-Matijevic model of scattered radiation intensity (J. OPTICAL SOCIETY OF AMERICA Vol 51, 1961), by using the minima of this indicatrix and the dependence of their angular positions on the fiber diameter. Numerical analysis of the scattering indicatrix for homogeneous dielectric cylinders 5-50 μm in diameter, calculations having been programmed in FORTRAN and covering 200 points within a 60° sector, reveals that the angular positions θ_{min} of the minima are descending oscillatory functions of the fiber diameter D. Only the $\theta_{min}(D)$ curve for the lowest-order minimum is continuous throughout the given range of fiber diameters. Those for successively higher orders are cut off at points corresponding to successively smaller diameters. Any one of these curves indicates the positions of different-order minima for different fiber diameters so that positions of successively higher-order minima are found by moving along a curve upward toward smaller diameters, while a cutoff indicates a step change in the angular position of the respective minimum. As the fiber diameter increases, these step changes pertain to higher-order minima. Within the range of small 0-10° scattering angles there appear intricate interference patterns distorted by interaction of diffracted and reflected radiation. The fringes become differently distorted as the fiber diameter changes, with additional minima of various magnitudes possibly but not necessarily appearing in the scattering indicatrix. Within the range of large 10-60° scattering angles the angular positions of the minima have been found to be monotonic and continuous functions of the fiber diameter, an approximately parabolic one $D = a\theta_{min}^2 + b\theta_{min} + c$ within the 10-30° range of scattering angles. This range therefore is the optimum one for measurement of small fiber diameters, requiring only that the values of coefficients a,b,c be known. They have been evaluated for the radiation wavelength $\lambda = 0.6328$ (He-Ne laser) and the refractive index $n = 1.457$ (quartz glass ?) on the basis of only seven $\theta_{min}(D)$ curves, sufficient for the required accuracy. Figures 1; tables 1; references 8.

UDC 681.586(042.3)

Acoustoholographic Robovision Sensors

917F0051A Leningrad IZVESTIYA VYSSHIKH UCHEBNYKH ZAVEDENIY: PRIBOROSTROYENIYE in Russian Vol 33, No 6, Jun 90 (manuscript received 26 Dec 89) pp 17-23

[Article by Ye. M. Yarichin, N. A. Shurygin, and V. M. Gruznov, Krasnoyarsk Polytechnic Institute]

[Abstract] Robovison sensors for visualization tasks, including three-dimensional visualization under conditions of cloudy or nontransparent media (smoke, a water

mass, metal, the human body, etc.), is one of the current directions in the development of spatial information sensors for robot systems. The development of nonoptical spatial information sensors is also linked to the development of spatial perception systems representing an alternative to complex multiple-camera television robovision systems. This article describes the architecture and sample hardware implementations of an acoustoholographic sensor for use as the main component of an acoustic robovision system intended to perform tasks related to remote spatial perception under conditions of media that are optically cloudy but that conduct sound. The acoustoholographic is based on a system bus that transmits data, data addresses, and control signals between the sensor's three units (a control processor, a receiving unit, and an irradiating unit). The control processor includes a central processor, a memory module (expanded RAM), and a peripheral control module that serves as an interface with standard peripherals and a special I/O module that constitutes the basis of an operator's workstation. (The function of the person operating the acoustoholographic sensor is reduced to tuning it much in the same way that an optical system is adjusted for sharpness.) The receiving unit (i.e., the unit recording the hologram) includes a multielement array that samples the acoustic field and a multiple-channel system to collect and record holographic information in digital form. The receiving module contains a section of the hydroacoustic array that consists of 16 piezoceramic elements and 16 identical wideband preamplifiers, each of which has a voltage-current converter, analog switch, and output buffer amplifier connected to its output. The acoustoholographic robovision sensor may also be implemented in the form of a single-frequency receiving unit or on the basis of a modular principle of organization. Under identical conditions, acoustoholographic robovision sensors provide a lower resolution than do optical robovision sensors, but they have a greater operating range. Figures 4; references 2 (Russian).

UDC [621.311.25:621.039]:65.016.8.004

Some Results of the Experience Accrued in Entombing the No. 1 Unit of the Beloyarsk AES

917F0059A Minsk ELEKTRICHESKIYE STANTSII in Russian No 11, Nov 90 pp 27-29

[Article by I.V. Vernitskaya, V.A. Makhov, and V.I. Platov (deceased), engineers, All-Union State Scientific Research, Planning, and Design Institute of Power Generation Systems and Electrical Networks, Ural Department, and Beloyarsk AES]

[Text] In addition to interacting with the environment in the manner characteristic of all thermal electric power power plants, nuclear power plants exert a radiation effect on the biosphere. The problem of nuclear and radiation safeguarding exists both in the period of a plant's operation and when it ceases operating, i.e., when the plant enters into a new economically unique state called removal from service. AES are taken out of service over a lengthy period during which a whole set of operations related to extracting fuel from reactors, entombment, deactivation, partial or complete disassembly of equipment and building structures, and sealing and burial of irradiated materials is implemented.

The absence in world practice of experience related to taking large power reactors out of service poses complex engineering problems for specialists in such areas as robotics and handing radioactive wastes.

In the initial stages of operation, technical and economic research is exceedingly important, especially for purposes of forecasting future indicators with respect to the branch.

Since the cost indicators of taking an AES out of service depend on the labor expenditures and method of conducting the operations, which are in turn determined by the initial radiation conditions in the live zone, the socially necessary expenditures related to taking AES units out of service are formulated on the basis of maximum reduction of the dose expenditures or aggregate irradiation doses incurred by personnel during the operations. By the year 2000 it will be necessary to take the following power plant units out of service: 100- and 200-MW units with water-cooled graphite-moderated pressure tube reactors at the Beloyarsk AES and two units with VVER-440 reactors at the Armyansk AES. The engineering experience accrued when taking these units out of service will make it possible to begin developments related to taking AES with RBMK-1000 and VVER-1000 reactors out of service in the future.

As the numbers of reactors taken out of service increases, methods must be developed to select rational versions of taking AES units out of operation with the purpose of optimizing expenditures throughout the branch.[1] One requisite of implementing such approaches is the presence of an information base that includes indicators related to ecological and economic assessment of the removal of this type of power plant unit from service.

An attempt was made to derive such indicators with consideration for the experience that has been accrued during the process of entombing the No. 1 unit of the Beloyarsk AES.

The No. 1 unit of the Beloyarsk AES was finally shut down on 18 July 1981. During its 17 years of operation it operated for 107,000 hours and produced 8 billion kilowatt hours of electric power. Work is underway to bring it into a long-term entombment mode in accordance with the plan of the NIKIET [expansion not given] and the Beloyarsk AES.

The required and actual labor expenditures and dose expenditures during the implementation of operations are very important indicators characterizing a power plant unit's status. Consolidated estimates of these indicators were made in a comparison of network models of charts of planned operations, and the estimate results have been fixed in reports.

Of the total labor expenditures for the period from 1981 to 1985, 32% were incurred to unload fuel. Of these, the maximum amount (57%) was incurred in 1983. The greatest intensity of the operations was observed in 1982 (amounting to 48%). Most of the labor expenditures in 1981-1982 were related to conducting labor-intensive operations related to repairing and redesigning the holding pond (BV-1) intended to store the fuel extracted from the reactor. A significant portion of the labor expenditures were related to the operations entailed in entombing the reactor that were conducted in 1983, including works to unload fuel. Analogous results were obtained with respect to the rem unit expenditure analysis. Most of the irradiation by personnel occurred during the operations related to unloading the fuel and repairing the BV-1.

An attempt was made to derive consolidated indicators that are intended to estimate—in prospective calculations—the volume of operations and capital expenditures entailed in taking power plant units with pressure tube reactors out of service. The following were adopted as such indicators:

—the specific labor expenditures related to one unloaded fuel assembly (in man-hours per unit);

—the specific capital expenditures related to entombing the unit (in rubles per kilowatt).

The dynamics of the labor expenditures incurred to extract one fuel assembly by years makes it possible to estimate the degree of increase in the labor intensity of work to extract wedged fuel assemblies versus undamaged fuel assemblies. The following calculation technique may thus be used for a consolidated estimate of the labor expenditures entailed in extracting fuel assemblies when taking high-capacity reactors out of service:

$$C_{ef} = K[(C^{un}_{ef} \times n^{un}) + (C^{w}_{ef} \times n^{w})],$$

where C_{ef} represents the total costs incurred in extracting the fuel, C^{un}_{ef} represents the specific labor expenditures with respect to extracting the undamaged fuel assemblies for the base reactor, n^{un} represents the number of undamaged fuel assemblies, C^{w}_{ef} represents the specific labor expenditures entailed in extracting fuel assemblies wedged in the reactor for the base reactor, n^{w} represents the number of wedged fuel assemblies, and K is a coefficient that allows for the change in labor expenditures with respect to extracting one fuel assembly for a design reactor versus the base reactor.

The labor expenditures entailed in extracting undamaged fuel assemblies and wedged fuel assemblies were determined for specific conditions on the basis of the experience accrued at the Beloyarsk AES (Table 1).

Table 1. Indicators by Year

Indicator	1981	1982	1983	1984	1985	1986
Labor Expenditures to Extract Fuel, man-hours	839	1,091	9,259	1,790	3,396	6,300
No. Unloaded Fuel Channels, units	84		621		26	
Specific Labor Expenditures to Unload 1 Fuel Channel, man-hours/unit	23		15		442	

As follows from an examination of Table 1, for the mass unloading of fuel assemblies (in 1983), the labor expenditures associated with extracting a single fuel assembly are not great, i.e., for AMB reactors they amount to 15 man-hours per piece. This indicator also includes an allowance for the auxiliary operations related to extracting fuel assemblies (the times required for work detail allowances, tool preparation, reconfiguration of cans with heat fuel assemblies into the holding pond, deactivation operations). The high specific expenditures to extract wedged fuel assemblies were determined by the development of the technology to extract them, which entails opening the reactor (disassembling the supporting tubes of the fuel assemblies and the steam and water communications and cutting out hatches in the upper plate of the reactor) and disassembling the reactor's combined masonry in the region of the wedged fuel assembly. In 1984-1986 this technology was used to extract 26 fuel assemblies; the specific labor expenditures to unload one fuel assembly increased by a factor of nearly 30 and amounted to 442 man-hours per piece.

These data regarding labor expenditures were used as the basis for determining the indicator specific capital expenditures for entombment. The specific yield was assumed to equal that in the branch, i.e., 10 rubles per man-hour. It should be noted that the quantity specific output allows for the cost of special reactor disassembly mechanisms, materials, and workers' wages plus overhead. The specific expenditures for entombment calculated for a kilowatt of installed capacity amounted to 5 rubles per kilowatt. Table 2 shows the values of the specific capital expenditures for the first stage of taking the No. 1 unit of the Beloyarsk AES out of service.

Table 2. Indicators by Year

Indicator	1981	1982	1983	1984	1985	Total 1981-1985
Capital costs to entomb AES unit:						
thousands of rubles	23.7	243.8	112.9	37.4	90.4	508.2
rubles/kW	0.2	2.4	1.1	0.4	0.9	5
including to extract fuel:						
thousands of rubles	8.4	10.9	92.6	17.6	34.0	163.8
rubles/kW	0.08	0.1	0.9	0.2	0.3	1.6

It should be noted that the amount of actual labor expenditures corresponds to their preliminary estimate. Because the experience of taking the No. 1 unit of the Beloyarsk AES out of service is the first in the USSR, the entombment operations are taking a long time. For the future period it is necessary to consider the size of the workforce required to complete the entombment in the shortest amount of time.

All of the operations related to entombment were performed by plant operating and maintenance personnel servicing the operational units in the period between repairs. This article gives a preliminary estimate of the numbers of personnel needed to entomb a unit by proceeding from the total doses received and the actual allowable irradiation dose per person, which equals 3 rem/yr (Table 3).

Table 3

Index	Year								Total 1981-1988
	1981	1982	1983	1984	1985	1986	1987	1988	
Total Dose Expenditure, rem	62	505	186	39	92	70	37	41	1032
No. Personnel Required to Entomb Unit, Persons	62	168	62	13	30	23	12	14	343

Assuming that the total dose expenditures for a five-year-plan are evenly distributed by year (177 rem/yr), approximately 60 persons are needed each year to conduct the entombment.

The peak number of personnel required in 1982, i.e., 168 persons, was on the order of the peak number required during disassembly of the reactor at the Shippingport nuclear plant in 1986-87, when between 250 and 300 persons working simultaneously were required for the operations entailed in disassembling the reactor.[2] Despite the fact that entirely different operations were performed at the Beloyarsk AES and the Shippingport plant, the adjusted comparison indicates that operations to take even low-capacity power plant units out of service require collectives of qualified specialists numbering in the hundreds.

Analysis of the data regarding labor and dose expenditures that were obtained during the entombment of the No. 1 unit of the Beloyarsk AES makes it possible to propose the existence of dependences between these units. Expert assessment of the dose expenditures required to conduct an entombment based on data from following the reactor at the moment it ceases operation and a calculation of labor expenditures on the basis of empirical dependences were performed during the conduct of consolidated calculations. In the future, when operations to remove units from service are conducted it will be necessary to develop a list of monitored indicators and methods of monitoring them. Without specifying an enormous amount of information to be established, it is necessary to ensure that the data required to develop consolidated indicators related to taking an AES out of service be obtained. One important type of information in this category is an accounting of the amount of radioactive wastes in accordance with the accepted classification and methods of measuring them. Only reliable volume and weight data regarding radioactive wastes in sealed form when an AES is taken out of service will permit correct a solution of the problems of transporting and burying them.

Conclusions

1. This work formulated the problem of making a consolidated estimate of the ecological and economic indicators of taking an AES out of service and creating the information base required to implement these operations in consideration of the domestic experience.

2. An approach to forecasting the labor expenditures incurred when entombing power plant units analogous to those at the Beloyarsk AES has been proposed on the basis of an analysis of data regarding entombing the No. 1 unit at the Beloyarsk AES.

3. The following are required with respect to further directions of operations on the theme under consideration:

—a search for consolidated indicators to adequately estimate the cost of operations entailed in entombing AES in the future;

—derivation of indicators with respect to the quantity of radioactive wastes and the cost of handling them in the stage of taking an AES out of service;

—development of the repair aspects of the problem of handling radioactive wastes in nuclear power generation.

References

1. V.A. Savchenko and S.N. Skovorodko, "Economic Aspects of Removing AES From Service," ATOMNAYA TEKHNIKA ZA RUBEZHOM, No 1, 1986.

2. V.A. Savchenko and S.N. Skovorodko, "Removing the Shippingport AES From Service," ENERGETICHESKOYE STROITELSTVO ZA RUBEZHOM, No 6,1985.

Preface to a Special Issue Devoted to Power Generation Development Strategies and the Chernobyl AES Accident

917F0102A Minsk IZVESTIYA AKADEMII NAUK BSSR SERIYA FIZIKO-ENERGETICHESKIKH NAUK in Russian No 4, 90 pp 5-6

[Article by A.A. Mikhalevich: "To Readers"]

[Text] Dear readers!

This regular issue of our journal differs from other issues from both a structural and content standpoint. It is almost entirely devoted to two problems that will be interconnected for decades to come: strategies for developing nuclear power generation and the accident at the Chernobyl AES. The importance and urgency of these problems for the modern world, our country, and our republic do not need to be argued.

This issue opens with an article by Prof. Ye.O. Adamov, with which we begin our scientific discussion of the problems of power generation. The article's author assesses the status of power generation in the country and proposes the concept of formulating a power generation program by examining the ecological, engineering, economic, social, and other aspects of the given problem. Although this journal's editorial board does not feel that it can make any evaluations, the fact that the ideas presented by this article's author, who is the chief designer of one of the main directions in the creation of AES in our country, are being implemented in actual practice with enviable energy and purposefulness must not be ignored.

As is assumed in a scientific discussion, the next article, which has been written by Prof. G.A. Sharovarov, contains a different view regarding modern power engineering and the possibilities of developing nuclear power generation. The authors of both articles are, however, in solid agreement regarding the fact that there is no real alternative to nuclear power generation in the foreseeable future. This journal's editorial board invites readers to continue this discussion in free form: to sent us not only basic articles but also concise communications and letters to the editor.

The fact that this issue's articles discussing the problems of the development of power generation are followed by the results of research related to eliminating the consequences of the accident at the Chernobyl AES was largely a coincidence in time. At the beginning of the current year, the Nuclear Power Generation Institute of the BSSR Academy of Sciences and the Nuclear Research Institute of the UkSSR Academy of Sciences reached an agreement regarding scientific-technical cooperation on the problem of eliminating the consequences of the Chernobyl accident. This agreement calls for exchange of experimental data, methods, mathematical programs, and specialists; conduct of joint seminars, working meetings, and annual scientific sessions on the problem; and publication of research results in the republic journals VESTSI AN BSSR, SERIYA FIZIKA-ENERGETYCHNYKH NAVUK and UKRAINSKIY FIZICHNYY ZHURNAL. Accordingly, we received a series of articles from our Ukrainian colleagues. Together with works completed at different organizations throughout Belorussia, these made it possible to present readers with so large a volume of scientific research results on this disturbing problem for the first time since the accident. Beginning with this issue, the rubric "The Problems of Chernobyl" will be a permanent rubric in our journal.

A.A. Sarkisov, corresponding member of the USSR Academy of Sciences, who has been put in charge of an office of the department of the physics engineering aspects of power generation at the USSR Academy of Sciences, analyzed the publications in our journal over the past years. He graciously agreed to the editorial board's requirement to present his opinion in the form of reviews, which we are placing at the end of this issue. Journal readers will undoubtedly be interested to learn the opinion that so well-known a scholar in the field of nuclear power generation has about our publications. We will note that the editorial board has already given consideration to one of his significant comments, i.e., the one regarding the absence of discussion materials, in this issue. We also intend to publish letters to the editor and introduce the respective rubric.

Abstracts From 'Bulletin of BSSR Academy of Sciences. Physics and Energy Series', No 3

917F0048A Minsk IZVESTIYA AKADEMII NAUK BSSR SERIYA FIZIKO-ENERGETICHESKIKH NAUK in Russian No 3, 90 pp 123-137

[Abstracts of articles appearing in "Bulletin of BSSR Academy of Sciences. Physical and Energy Sciences Series," No 3, 90]

[Text]

UDC 621.039.534

The Possibility of Express γ-Spectrometric Control of the Boron Content in the Coolant of a VVER Reactor Based on Recording the Instantaneous γ-Quanta of ^{7}Li Nuclei. M. L. Zhemzhurov, V. A. Levadnyy, and A. A. Lukhvich, pp 3-10

This article examines the possibility of measuring the ^{10}B content in the coolant of a water-moderated water-cooled [VVER] reactor by the γ-spectrometric method based on recording the instantaneous radiation of excited ^{7}Li nuclei generated in a flow of circulating coolant under the effect of neutron activation of ^{17}N. Calculated dependences linking the boric acid concentration in the primary loop to the ratio of recording activities of the isotopes ^{7}Li and ^{16}N are derived. Tables 3, references 12.

UDC 621.039.51

Stochastic Modeling of the Near-Critical and Critical Behavior of Nuclear Reactors. , R. V. Boyko and V. V. Ryazanov, pp 10-16

By using the theory of branching random processes with a variable mode and with immigration, the authors construct a stochastic model of the operation of a nuclear power reactor in the vicinity of its critical mode. They determine operating modes depending both on the reactivity of a zero-capacity reactor and on the reactivity induced by control, feedbacks, and immigration of neutrons into the system. Expressions coordinated with the fractal geometry of neutron trajectories and the general theory of critical processes are derived for the critical behavior of a nuclear reactor. Explicit stochastic characteristics of a nuclear reactor are derived that expand the domain of the determinate description of reactor systems. References 9.

UDC 621.039.58:519.217

Using a Markov Model To Estimate the Reliability of AES Equipment. E. B. Pereslavtsev and I. V. Saltanova, pp 17-20

This article examines forecasting the reliability parameters of a local control system for AES equipment. A mathematical model of a system to control the operation of compressors is constructed within the framework of the analytical engineering approach. The performability of such a diagram is calculated. The system's functioning is examined in the form of a markovian process. The control algorithm is used as the basis for plotting the system's state graph. The resultant system of differential equations is integrated numerically with satisfactory precision. Numerical values are obtained for the following reliability parameters: availability, failure flow index, mean time between failures, and average recovery time. Figures 2, references 3.

UDC 621.039.51

Improving the Safety Characteristics of Fast Reactors by Using Thorium and ^{233}U. V. M. Murogov, V. Ya. Rudneva, A. I. Stavrov, and K. N. Zhulanova, pp 20-24

This article presents the results of mathematical research on different types of reactors, i.e., type BN-350 low-power reactors and type BN-1600 high-power reactors based on oxide and metal fuel. The results of a comparison of the main breeding indicators and selected safety characteristics for different fuel composites are summarized. The research showed that using ^{233}U and thorium makes it possible to improve the safety characteristics of reactors based on oxide and on metal fuel. The possibility of improving the safety characteristics of uranium-plutonium reactors by introducing ^{233}U into the core was investigated. Tables 3, references 8.

UDC 628.334.15

Conditioning Wastewater Residues Under the Effect of Ionizing Radiation and Oxidizing Agents-Reagents. Ye. P. Petryayev, V. G. Shlyk, A. A. Sosnovskaya, V. G. Nalivayko, N. B. Yanchik, pp 25-29

This article investigates the effect of hydrogen peroxide, aeration, and γ-radiation on the water yield of raw sediment (that has been acidified to a pH of 2.6-3.3) from primary settling tanks and excess activated sludge. It is established that irradiation with simultaneous aeration makes it possible to improve the filterability of sediments by a factor of 20-26 and to decontaminate them. The optimum treatment modes (dose, air flow rate, pH) are found. A method is proposed for conditioning sediments by treating them with ionizing radiation at a dose of 0.4-0.5 kGy and with hydrogen peroxide in a concentration of 0.007-0.1 M. Such treatment improves filterability by a factor of 100-200 and results in effective decontamination. Figures 3,references 12.

UDC 504.06:621.311.25:621.039

Problem of the Maximum Ground Concentration of Radionuclides During Emission Into the Atmosphere. G. M. Zhmura, Ye. F. Kislyakov, and S. B. Kulich, pp 29-34

This article investigates the effect of the flow rise on the maximum allowable concentration of radionuclides with an allowance for depletion of the cloud on account of radioactive decay and "dry" precipitation. It is shown that allowing for the rise of the flow may result in a reduction in the maximum allowable concentration by an order of magnitude for the main isotopes released by AES and has a significant effect on emission characteristics that are important when calculating the radiation conditions at a location. Table 1, figures 3, references 6.

UDC 541.15:628.334.15

Treating Wastewater Sediments With Accelerated Electrons. A. A. Sosnovskaya, N. N. Subbotina, G. M. Vasilevskiy, and M. F. Denisenko, pp 34-35

This article presents research on treating the sediments of stations conducting biological treatment of wastewaters by accelerated electrons. The possibility of reducing the neutralizing dose of accelerated electrons by adding chemical reagents before irradiation is demonstrated. Other techniques for reducing energy expenditures to treat wastewater sediments by accelerated electrons are examined. References 3.

UDC 621.81:539.4.001.24(035)

Estimating the Survivability of a Reactor Vessel Model. L. A. Sosnovskiy, pp 36-40

This article proposes and implements a scheme for calculating the fatigue strength of a model of a reactor vessel that has been manufactured from ductile steel and that has a crack. Tables 2, figure 1, references 7.

UDC 539.12

Effect of a Weak Pseudomagnetic Field on the Oscillation of Neutrino and Collective Processes in Supernova Matter and Neutrino Gas. V. G. Varyshevskiy, pp 41-45

This article demonstrates that a non-zero degree of polarization of the matter of a supernova results in precession of a neutrino's spin, even if the neutrino's magnetic moment equals zero. Such precession may turn out to have a noticeable effect on the dynamics of a supernova. References 9.

UDC 539.121.8

Optical Modulation of a Relativistic Electron Beam During Three-Wave Parametric Interaction. L. D. Karas, pp 45-49

An equation system for three parametrically associated waves that describes the nonlinear interaction of a relativistic electron beam with an electromagnetic wave falling counter to the beam's motion is derived from Maxwell equations and the motion equation of a relativistic electron beam. The equation system derived is solved numerically in order to find the modulation depth of the beam's density. It is shown that any modulation depth is allowable during continuous pumping. Figure 1, references 8.

UDC 621.378.325

X-Ray Laser Based on Free Electrons in a Crystal Cavity With Distributed Feedback. V. G. Baryshevskiy, I. Ya. Dubovskaya, and A. V. Zege, pp 49-56

This article constructs a theory of a relativistic laser based on free electrons in a crystal cavity with distributed feedback and derives a variance equation for its radiative instability. The lasing thresholds are found, and their magnitude is estimated. Electromagnetic and magnetostatic wigglers are examined. It is concluded that using a non-one-dimensional geometry is important. Estimates show that increasing the beam's brightness by a factor of 20 as compared with that in existing accelerating systems is sufficient to meet the lasing conditions. Tables 2, references 11.

UDC 533.6.011

Conditions of Equalizing Radial Flows in Header Systems. N. N. Suntsov, S. L. Demenok, and A. I. Gusev, pp 57-62

This article presents a theoretical analysis of the conditions of equalizing transverse coolant flows in a Z-shaped header apparatus. A mathematical model of the two-dimensional motion of coolant in the header system is developed on the basis of the hypothesis of constant vorticity along the current line (for a distributing header, the model is based on an approximation of the boundary layer; for a collecting header, it is based on an approximation of the potential flow). Analysis of the resultant solution indicated that even distribution of coolant along the header system's length may be accomplished by taking design measures related to artificial organization of the introduction of coolant into distributing and collecting headers. Figures 2, references 8.

UDC 536.423.4.001.5:621.039.534.3

Experimental Research on Heat Transfer During the Condensation of Nitrogen Dioxide Vapor From an NO_2-NO-N_2 Vapor and Gas Mixture in a Bundle of Horizontal Tubes With Annular Knurling and Heat Transfer in Dynamic Two-Phase Layer With Different Cooling Surfaces. L. I. Kolykhan, V. F. Pulyayev, and A. V. Sharyy, pp 62-68

This article presents the results of a complex of experimental research on heat transfer during the condensation of nitrogen dioxide vapor from an NO_2-NO-N_2 mixture in models of surface- and drum-type condensers. the intensity of heat transfer during condensation in different models increases as the flow velocity increases. In drum-type condensers it is virtually independent of the condensation temperature heads and mass content of noncondensed NO + N_2, whereas in the case of film-type condensation on a bundle of horizontal tubes it is decreased by about $c_{NO+N2}^{-0.25}$. The specific thermal during condensation in tubes with annular knurling is about 20-30% higher than in smooth tubes. This is due to the principal effect of the turbulizing flanges along the side of the cooling water.

The research results are presented in the form of generalizing dependences that are recommended for calculating heat transfer during condensation of the vapors of different substances in the types of headers examined. The comparative characteristics of surface- and drum-type experimental condensers are presented. Tables 2, figures 3, references 9.

UDC 621.0395

Experimental Investigation of a VVR-M5 Fuel Assembly in Air. N. A. Grosheva, G. A. Kirsanov, K. A. Konoplev, and Zh. A. Shishkina, pp 68-72

This article presents the results of measuring the temperature of the fuel elements of a type VVR-M5 fuel assembly in air as a function of time and energy release capacity. The research was conducted on a model fuel assembly with electric heating for a fuel assembly suspended vertically and lying on a heat-insulated support.

The experiment results were approximated by simple empirical dependencies permitting quick calculation of the temperature of the hottest fuel element in the energy release range from 10 to 90 W during operations connected with the extraction of a fuel assembly in air. Figures 3, references 2.

UDC 536.422.4:532.54

Intensive Nonuniform Sublimation of the Inner Coating of a Slit Channel's Walls. L. Ya. Lyubin and V. I. Novikova, pp 73-80

This article examines compressible flows characterized by large relative pressure differentials with bulk condensation of the compressible medium occurring in plane slit channels during sublimation of the inner coating of the walls.

An approximate method of solving the problem is proposed. The current lines and pressure distribution, longitudinal component of the velocity, and mass density of the sublimate in the cross sections of a plane channel are calculated. Figures 4, references 8.

UDC 532.55:536.422.4

Gas Flow in Slit Channels With Isothermal and Adiabatic Conditions in Permeable Walls. L. Ya. Lyubin and V. I. Novikova, pp 80-86

This article examines a flow of compressible gas in slit plane and steplike channels formed by porous walls for the case of isothermal and adiabatic conditions in them.

A method for an approximate solution of the problem is proposed, and the pressure differential, current lines, and distribution of the longitudinal velocity component along plane and one-step channels given different-size steps and Mach numbers are calculated. Figures 3, references 4.

UDC 532.58:537.612

The Motion of Drops of Magnetic Liquid in a Nonuniform Magnetic Field. V. I. Bakalenko, A. N. Vislovich, and V. F. Medvedev, pp 86-90

This article examines the motion of drops of a magnetic liquid in the nonuniform field of a magnetic separator. An approximate linear-fractional function is used in describing the magnetic liquid's magnetization curve. An analytical connection between the elongation of the drop of magnetic liquid and the intensity of the magnetic field is obtained. The calculated dependences are confirmed experimentally. The results presented in the article are the theoretical basis for a method of engineering calculation of the overall dimensions of the live zone of a magnetic drop separator. Figures 3, references 10.

UDC 621.039.517.5

Optimization of the Channel Profiles of a Radial-Type Device With Allowance for the Precision of Their Manufacture Guaranteed by Manufacturing Technology. A. P. Akhramovich, V. P. Kolos, and V. N. Sorokin, pp 90-101

On the basis of the existing model of the thermohydrodynamics of a radial-type fuel assembly, methods of the linear theory of perturbations and the calculus of variations are used to derive a system of first-order ordinary differential equations that are solved in relation to their derivatives. Also derived are those boundary conditions describing the profiles of the distributing and drainage channels for which the error of the empirical formulas used in the calculations and the imprecision of manufacturing the channels themselves cause the minimum deviation of the real distribution of coolant along the length of the fuel layer from the desired distribution.

A comparison is presented of the energy intensities of carbon dioxide-cooled devices calculated on the basis of the method developed and the existing method, which is oriented toward achieving maximum compactness of configuration. The results of the numerical experiments are used to substantiate an optimum capacity of 400 MW for the device. Figures 3, references 16.

UDC 536.24

Mathematical Model of a Loop With Natural Circulation and an Exterior Cooling Loop. V. G. Kompel and A. P. Yakushev, pp 102-106

This article proposes a mathematical model for calculating the heat transfer characteristics and hydrodynamics in a loop with natural circulation in the case of a steady turbulent flow of compressed gas. A numerical investigation of the dependence of the flow rate of the coolant in the loop on the heater's capacity, the flow rate of cooling liquid, and the width of the downcomer gap in the heating section is presented. Figures 3, references 13.

UDC 681.3:62-135:533.6.011

Finite Element Method of Calculation of the Circulation of a Lattice of Profiles With a Transition Through the Speed of Sound. L. A. Dorfman and A. Z. Serazetdinov, pp 106-110

This article describes the use of the finite elements method in calculating a steady transonic flow in plane lattices of the turbomachine profiles. A grid of triangular elements with nodal points at the vertices is used. An "artificial" compressibility is introduced for the transition through the speed of sound. This makes it possible to obtain reliable results up to value of M = 1.3 to 1.4 on a profile. Sample calculations show that the finite element method calculations are in good agreement with calculations for a determination when $\lambda_{max} = 1.08$ but are somewhat worse when $M_2 = 0.5$. Calculations based on the finite element method require much less computer time. Figures 3, references 5.

UDC 533.27:621.981.92

Determining Concentration Derivatives From the Gibbs Energy of Binary Gas Mixtures by the Method of Pressure Diffusion Separation of Their Components in a Centrifugal Force Field. L. S. Kotousov and A. B. Korolev, pp 111-115

This article investigates the difference between real binary gas mixtures and the same types of ideal mixtures by using the reduced function y_i^*, which is determined by the second concentration derivative of the Gibbs energy. This function is calculated on the basis of the measured effect of the pressure diffusion separation of binary gas mixtures in the pressure range up to 5,000 Pa and at a temperature of 17 to 30°C in a centrifugal force field.

The results obtained are in good agreement with the results of the previous work on pressure diffusion separation of binary gas mixtures in a gravity field. A comparison with the theory of pressure diffusion shows that the separation effects found are severalfold greater

than for the respective ideal systems. The second concentration derivatives of the Gibbs energy are determined. They are in good agreement with values obtained previously on the basis of thermodiffusion analysis. Figures 3, references 4.

UDC 536.3:535.312

Method of Calculating the Heating and Temperature Stress in Tube Reflectors When They Interact With a Unilateral Heat Flow. V. V. Klubovich, A. A. Pivovarchik, G. P. Maltsev, and Ye. I. Konoplev, pp 116-119

The heating and temperature stress in tube reflectors under the effect of a unilateral heat flow is calculated. It is shown that the temperature distribution is asymmetrical relative to the plane zOy and that, consequently, the temperature field causes a torque that is constant along the length of the tube, with the greatest axial tensile stress occurring in the cross sections of the middle section of the tube. Figures 2, references 2.

Abstracts From 'Bulletin of the BSSR Academy of Sciences. Physics and Energy Series', No 4

917F0102B Minsk IZVESTIYA AKADEMII NAUK BSSR SERIYA FIZIKO-ENERGETICHESKIKH NAUK in Russian No 4, 90 pp 124-128

[Abstracts of articles appearing in "Bulletin of the BSSR Academy of Sciences, Series Physics Engineering Sciences," No 4, 90]

[Text]

UDC 621.039.58

Nuclear Power Generation: Its Safety, Economy, and Place in the Country's Energy Balance. Ye.O. Adamov, pp 7-18

This article examines the main problems in formulating a strategy for the development of nuclear power generation in the USSR: the accident at the Chernobyl AES, the small percentage of electricity products by AES in the country's energy balance, the transition of the country's energy economy to real resource conservation, the removal from service of electric power plants that have outlived their useful life, the development of alternative energy sources, etc. This article shows the effectiveness of measures to increase the safety of RBMK reactors that were taken after the accident for the purpose of reducing the steam reactivity coefficient, increase the speed of and create independent emergency protection, and develop equipment automatically preventing a reactor's operation in the event of deviations from requirements specified in regulations. The prospects for the next stage in the development of nuclear power generation are examined, and the requirements regarding the creation of new-generation AES are analyzed. Tables 2, figures 9.

UDC 621.039.58

The Problems of Power Generation Safety. G.A. Sharovarov, pp 18-22

This article examines the causes for the energy crisis caused by the increase in energy consumption. Different energy sources are analyzed. It is shown that the energy of the nucleus is the only real energy source. The difficulties in safeguarding nuclear power generation are indicated. Data regarding the dynamics of the Chernobyl accident are presented. References 3.

UDC 63:621.039(476)

Selected Results of Research on the Effect of Radioactive Contamination of Agricultural Lands in Belorussia. I.N. Nikitchenko, pp 23-30

This article analyzes the results of monitoring the contamination of Belorussia's agricultural lands after the Chernobyl catastrophe. The resultant data are used as the basis for recommendations regarding safe conduct of agricultural production and are used in developing the State Program To Eliminate the Consequences of the Accident at the Chernobyl AES. Tables 4.

UDC 616.001.28:577.391

Biological Effects of the Combined Action of Radiation and Chemical Factors. A.F. Malenchenko, pp 30-38

This article examines the problems of the multifactorial nature of the effects that environmental pollutants exert on the body and on possible alteration of its immune response: additivity, synergism, and antagonism. Possible practical solutions regarding improving the ecological situation and reducing the risk of the negative consequences of anthropogenesis are analyzed. Tables 2, references 14.

UDC 539.12.08

"Hot" Particles in the Biosphere. L.G. Borisyuk, V.I. Gavrilyuk, I.S. Dotsenko, A.I. Yermakov, N.N. Zhdanoa, A.V. Kovalev, T.N. Lashko, P.N. Muzalev, T.I. Redchits, O.I. Sinyavskaya, and A.A. Ter-Saakov, pp 38-41

This article presents the first data regarding studying the effect of the biosphere, specifically, coil micromycets, on the process of the breakdown of "hot" particles formed as a result of the accident at the Chernobyl accident.

On the basis of preliminary data, it is established that intensive breakdown of "hot" particles connected with the vital activity of soil micromycets is observed in a model experiment. Figures 2, references 6.

UDC 541.539.163

Occurrence of "Hot" Particles in the Southern Regions of Belorussia. Ye.P. Petryayev, G.A. Sokolik, S.L. Leyrova, Ye.M. Danilchenko, and M.A. Kazantseva, pp 42-49

This article presents results characterizing the distribution of active particles in the soils of the Gomel and Mogilev oblasts located distances of 40, 200, and 250 km from the site of the accident. It is shown that the number of particles depends on the distance to the contamination source and decreases from 10^5 to 10^3 per square meter as the distance from the Chernobyl AES increases. The nature of the distribution of active particles in air is analogous: The closer to the site of the accident, the more particles there are, and the greater their contribution to the total β-activity.

It is discovered that the most of the active particles are generally located in the 0- to 1-cm layer of soil, i.e., they are practically on its surface. The nature of the distribution of particles throughout the depth of the soil resources does not depend on the distance from the contamination source; rather it is mainly determined by the type of soil. It is noted that particles enriched with ruthenium, cerium, and cesium are among those active particles encountered. As the distance from the Chernobyl AES increases, an increase in the amount of cesium-enriched particles is observed. Tables 7, figures 3, references 5.

UDC 551.515.3

Effect of the Secondary Wind Lifting and Transfer of Radioactive Particles on Air Pollution. M.A. Drugachenok, V.P. Mironov, and V.I. Makarevich, pp 50-53

This article presents the results of observations of radioactive fallout in the Khoynikskiy rayon of the Gomel Oblast at the end of April 1989. It is shown that the lifting and transfer of radioactive particles from the underlying surface makes a significant contribution to the near-ground air in regions adjacent to the 30-km zone of the Chernobyl AES. The intensity of wind lifting is estimated for the surface of a natural meadow that is uniform with respect to its horizontal surface. Figures 3, references 4.

UDC 501.06:621.311.25:621.039

Estimating Pollution of the Near-Ground Atmosphere by Cesium 137 During the Dusting of Site Sources. A.P. Bogdanov, V.N. Doroshkevich, G.M. Zhmura, and V.A. Petrov, pp 53-58

An expression for calculating near-ground concentrations during the dusting of a rectangular site source is derived within the framework of a gaussian statistical model by using the principle of superimposition for point sources. Also derived are an expression for calculating the mean yearly ground concentrations of radionuclides during the dusting of a round site source and an analytical expression for estimating the mean yearly ground concentrations of ^{137}Cs. Results of mean yearly ground concentration and ground concentration calculations for ^{137}Cs are presented. Table 1, figures 3, references 7.

UDC 621.039.580.38

Dose Characteristics of β-Radiation Leaving the Surface of Radionuclide-Contaminated Soil. A.P. Bogdanov, P.V. Bulyga, M.V. Bychkov, and O.M. Zhukova, pp 58-60

The absorption method is used to conduct an experimental study of the energy characteristics of β-particles from the surface of soil contaminated with radionuclides. The effective values of the threshold energy of a complex β-spectrum are calculated.

A method is proposed for calculating the dose characteristics of β-radiation, and the need to consider the β-radiation dose to the skin as a critical organ for individuals in a zone of radionuclide contamination is demonstrated. Figure 1, references 3.

UDC 621.039.58

Problem of the Forms in Which ^{137}Cs and ^{144}Ce Radionuclides Are Located in the Soils of Belorussia. Yu.P. Davydov, N.I. Voronik, N.N. Shatilo, T.V. Vasilevskaya, and I.V. Kupriyanova, pp 60-65

This article presents a method for and the results of research on the behavior of ^{137}Cs and ^{144}Ce radionuclides that ended up in soils as a result of the accident at the Chernobyl AES and the behavior of these same radionuclides when they are added to the same soil in ion form.

It is shown that the amount of desorption of ion forms of radionuclides (in model experiments) is very different from the amount of desorption of those radionuclides that ended up in the soil as a result of the accident. A disperse state of those radionuclides that fell onto the soil after the accident is concluded on the basis of these data. Tables 2, figures 4.

UDC 541.15:539.163

The Forms in Which Radionuclides Are Located in the Soils of Contaminated Regions of Belorussia. Ye.P Petryayev, S.V. Ovsyannikova, I.Ya. Lyubkina, and S.Ya. Rubinchik, pp 65-69

The method of selective dissolution is used to study the forms of those radionuclides that are in the soils of the southern regions of Belorussia because of accidental emission from the Chernobyl AES.

The relationship between water-soluble, exchange, acid-soluble, and strongly bound forms of the isotopes ^{134}Cs, ^{137}Cs, and ^{90}Sr in 1-cm layers of soil at different depths from the surface is established.

It is shown that most of the radioactive cesium is located in a "fixed" state. The isotope ^{90}Sr is present in the soil mainly in exchange and "fixed" states. It is found that the amount of exchange radioactive strontium increases in most cases, whereas that of the "fixed" radioactive strontium moderates as the distance from the contamination source increases. In deeper soil layers, the fraction of radionuclides in a exchange state generally increases.

The experimental data obtained confirm the higher migration capability of ^{90}Sr isotopes as compared with ^{134}Cs and ^{137}Cs. Tables 5, references 6.

UDC 539.12.08+681.3.4

Change in Contamination Levels of the 30-km Zone Around the Chernobyl AES. V.A. Zheltonozhskiy, S.V. Kazakov, T.N. Lashko, P.N. Muzalev, Ye.D. Stukin, A.K. Sukhoruchkin, A.V. Shustov, and A.M. Shcherbachenko, pp 69-73

This article studies the distribution of the main radionuclides within a 30-km radius from the Chernobyl AES, with the exception of the 5-km zone around the plant. Programs are developed for mapping with a regular "angle-distance" grid. Isotope charts are plotted. The reserve activity of ^{144}Ce and ^{137}Cs under specified isoline values and throughout the entire 30-km zone are determined. Tables 2, references 2.

UDC 539.163:631.42

Assessment and Forecasting of Radioactive Contamination of the Soil Cover of the Southern Regions of Belorussia. Ye.P. Petryayev, G.A. Sokolik, T.G. Ivanova, T.K. Morozova, N.I. Kovalenko, and G.K. Glushonok, pp 73-77

This article presents a comprehensive study of radioactive contamination (the density and isotope make-up of fallout and the distribution of radionuclides throughout the depth of the soil profile) at 12 stations in three geochemical/landscape test sites within a radius of 40 to 250 km from the Chernobyl AES. The migration capability of radionuclides (cesium 134, cesium 137, ruthenium 106, cerium 144, and strontium 90) in the soil and plant cover is studied. Computer programs are used for mathematical processing of the experimental data in order to estimate the rate parameters and compile a forecast of the migration of radionuclides. The calculated values of the migration coefficients range from 0.4 to 10 x 10^{-8} ($cm^2 \times s^{-1}$) for slow-migrating components and from 10 to 90 x 10^{-8} ($cm^2 \times s^{-1}$) for fast-migrating components. A long-range forecast (5 to 50 years) of the distribution of radionuclides in the soil profile is used to estimate the values of the effective half-life. A low degree of ground water contamination is forecast for the coming decade. Tables 2, figure 1, references 10.

UDC 541.15:539.163

Change in the State of Radionuclides in the Contaminated Territory of the BSSR. Ye.P. Petryayev, S.V. Ovsyannikova, G.A. Sokolik, S.Ya. Rubinichik, and I.Ya. Lyubkina, pp 78-83

The method of sequential selective leaching is used to study the forms in which radionuclides from the accidental emission from the Chernobyl AES are located in the soils of isolated stations located within the territory of Belorussia at a distance fo 40 to 250 km from the reactor.

The relationship between water-soluble, exchange, mobile, and "fixed" forms of the isotopes cesium 134, cesium 137, and strontium 90 in soddy meadow, soddy-podzolic, and peaty bog soils is established.

The change in the relationship between the specified forms of radionuclides over time and throughout the depth of the soil is studied as a function of the distance to the accident site.

It is established that most of the radioactive cesium in the soil is in a strongly bound state. The relationship of its forms does not depend on the distance to the Chernobyl AES. The vertical migration of cesium isotopes in the soil occurs mainly on account of the "fixed" form.

Most of the radioactive strontium is distributed between the exchange and "fixed" states. The relationship of the forms of strontium 90 is very dependent on the distance to the site of the accident. The vertical migration of radioactive strontium in the soil occurs primarily in exchange form.

The mobility of strontium 90 in all sections exceeds that of the radioactive cesium isotopes and, in a number of cases, increases with time. Tables 2, references 11.

UDC 621.039.76

Determination of the Correlation Between the Activity of ^{239}Pu and ^{240}Pu with ^{144}Ce and ^{106}Ru in Soil Specimens From a 30-km Zone Around the Chernobyl AES. L.V. Sadovnikov, L.I. Bernadina, V.I. Gavrilyuk, A.N. Masko, S.V. Nederya, G.N. Pshinko, A.V. Shustov, and A.M. Shcherbachenko, pp 83-87

The correlation coefficients and ratios of the activity of the isotopes ^{239}Pu and ^{240}Pu to that of ^{106}Ru and ^{144}Ce are calculated by using the method of statistical regression analysis based on experimental data. The stability of the correlation with a confidence level of 0.9 is shown for the northern section of the 30-km zone surrounding the Chernobyl AES. Tables 2, figure 1, references 3.

UDC 539.12.08+691.3.4

Problem of the Transfer of Radionuclides Originating From the Chernobyl AES Into Agricultural Plants in the Territory of the Northern Rayons of the Ukraine. L.I. Bernadina, V.A. Vetrov, V.I. Gavrilyu, and R.N. Oleynik, pp 87-92

This article examines the contamination of agricultural plants by Chernobyl radionuclides in a network of agroecological test sites organized so as to encompass the most diverse soil and climate conditions and agricultural crops possible. Generalized characteristics of radioactive contamination of agricultural plants are derived and presented in the form of accumulation coefficients and transition coefficients. The values of the coefficients vary within broad limits. Reliable boundaries of the transition coefficients are derived for the most typical versions of the system soil-plant. The average values of K_{tran} are obtained; they reflect the dynamics of contamination of most commercial horticultural products in two soil and climate zones of the Ukraine. The results are presented in table form. Tables 2, figure 1, references 3.

UDC 539.12.08

Study of the Distribution of the Density of Contamination of the Polesskoye Urban-Type Settlement by Long-Lived Radionuclides. A.I. Yermakov, A.G. Zhidik, S.V. Kazakov, T.N. Lashko, P.N. Muzalev, L.V. Sadovnikov, V.B. Kharlanov, A.V. Shustov, and A.M. Shcherbachenko, pp 92-97

About 1,500 samples of the environment in the Polesskoye urban-type settlement were collected and examined. The distribution of the principal radionuclides was studied. It was established that most of the activity in the arable lands is at a depth of 20-25 cm.

An applications package for mapping the distribution of radioactivity in a site with an irregular sampling grid is developed. The distribution of total radioactivity is also plotted for ^{137}Cs.

The results of this work are important for forecasting dose loads on inhabitants of the Polesskoye urban-type settlement and for estimating the amount of decontamination work required for radiation safeguarding. Tables 2, figures 2, references 8.

UDC 539.12.08

Automated System for Spectral Measurements and Analysis of the Content of γ-Radionuclides in Objects in the Environment. L.I. Bernadina, V.I. Gavrilyuk, V.A. Zheltonozhskiy, V.V. Zerkin, T.N. Lashko, P.N. Muzalev, S.V. nederya, V.D. Stetsenko, V.B. Kharlanov, A.V. Shustov, and A.M. Shcherbachenko, pp 98-105

An automated system based on an SM-1420 minicomputer and NOKIA LP-4900 B multichannel analyzer that makes it possible to measure the γ-spectra of samples, input accompanying information, and calculate and print measurement results and summary tables has been developed at the Nuclear Research Institute of the UkSSR Academy of Sciences. It was especially created for work connected with the problem of the accident at the Chernobyl AES. An applications package for use in mapping radioactive contamination of the site has been developed for the system.

A cycle of work based on the Reper program has been conducted by using the system in a 60-km zone around the Chernobyl AES. Figures 4, references 9.

UDC 539.071

Precision Ge(Li)-Detectors Used in Radioactive Element Analysis of Low-Activity Samples. V.I. Gavrilyuk, I.G. Kirnas, E.Ye. Petrosyan, N.N. Pashchuk, N.S. Petrenko, and S.V. Nederya, pp 105-107

It is shown that by controlling the concentration of uncompensated acceptors in the sensitive range of Ge(Li)-coaxial detectors during the process of equalizing drift one can obtain the required value of the intensity of the electrical field and its even distribution throughout the entire volume of the detector and, consequently, improve its spectrometric characteristics. Figures 2, references 2.

UDC 536.24

Method of Allowing for Preliminary Cooling in a Physical Model of Repeated Wetting. L.P. Kabanov, R.Kh. Khasanov, and Din Chuk Nam, pp 107-115

This article presents a method of allowing for preliminary cooling when determining the dimensionless velocity (Re) of a conductive-convective repeated-wetting front in regard to the process of emergency flooding of the core of water-cooled nuclear reactors. A systematic experimental study of steel and zirconium pipes is used as the basis for deriving a dependence for determining the integral of the thermal flux released in a zone of preliminary cooling. In the absence of preliminary cooling, the Re calculation mode is transformed into a two-dimensional analytical Du [transliteration] and Ten [transliteration] solution for Re obtained with no allowance for preliminary cooling. Figures 2, references 14.

UDC 678.034:621.98

Inertialess-Drive Robotized Flexible Integrated Transport Systems

917F0112A Moscow
KUZNECHNO-SHTAMPOVOCHNOYE PROIZVODSTVO in Russian No 11, Nov 90
(manuscript received 11 Jan 90) pp 24-26

[Article by N.V. Potekushin, candidate of technical sciences, and F.A. Krasin]

[Text] Integrated robotized flexible transport systems having various configuration modifications have been developed and mastered by the Chelyabinsk Organic Glass Plant and have been successfully implemented. The principal design-uniting functional component of each system is a built-in process-specific manipulator robot (fig 1).

The surface-mobile, elevating and pivoted, stationary and versatile- rotation robot having an individual inertialess electric drive lumps together actuating, transfer and locomotion—principal and secondary—functions.

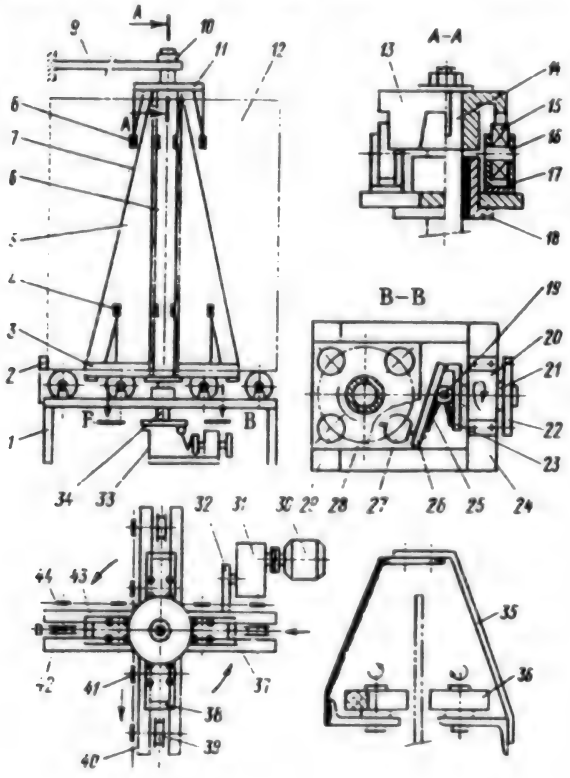

Figure 1. Sketch of Separator Elevating and Pivoted Manipulator Robot

The lower semiaxle, 34, with the frame-type separator's, 5, flat, square driven diaphragm, 28, which has four identical (35 mm in diameter) round holes—holes 29, is cantilevered in a (lower) solid sleeve bearing, at the intersection of the plane axes of a rectangular cross-shaped supporting and power-driven mounting base, 1. The semiaxle is extended by a vertical structural frame, 6, having, oriented relative to one another, a cross, 3, and plate-like disk, 11, and having oblique braces, 7, that impart strength and stability to the four-quadrant separator. The frame ends in an upper reinforced cylindrical semiaxle, 14, which makes contact with a holder bracket, 9, and the positioning index head, 10, of the separator.

The receiving and extension sections of the cross are covered by end and intermediate transverse supporting plates, 37 and 38. The separator has four pairs each of lower, 4, and upper, 8, guide and adjusting idler (cylindrical, rod-type, barrel-type, etc.) rollers made of SKU-7L polyurethane. The intervals (horizontally) and distance (vertically) between the rollers are changed and adjusted based on the dimensions of the vertically positioned sheet blank (semifinished product, part), 12. Functional identity and geometrical invariance of the rollers are achieved by various design modifications of them, e.g., a design for spontaneous rollers, 36, in the form of a disk enveloped by half-frames, 35.

The moving positioning index head is detachable. Guide (centering) bushing 18, with a fixed plain bearing shell, is press-fitted into a bracket beneath the upper semiaxle or into an additional horizontal gasket. Two antifriction bearings, 15, playing the role of contact orienting and checking thrust-bearing locators, are placed on axles 16 diametrically to the semiaxle in rigid upright races, 17. Four lateral open grooves of a specific shape with slanting walls, evenly distributed over the perimeter, are provided in the outer wall of the highest- quality master cam, 13, connected to the semiaxle. Each pair couples alternately with the bearings the same way as in a single-pair gearing.

Grooved intercoordinated metal drive rollers, 39 and 42, with two-sided rims are placed on individual axles in the parallel-in-pairs crossing beams, 40 and 43, identically to the arrangement of the flexible guide rollers. The arms of the axles in the axle supports are coupled by means of driven sprockets 41 and 44 with the common traction chain drive of the feeding and receiving (detachable) roller conveyers (not shown in fig 1). A stop, 2, with an electric limit switch projects above the rollers on the side opposite the feeding (according to the arrow) roller conveyer.

An emergency stopping device, 33, for the diaphragm and a coordinated sleeve bearing, 20, with a take-on shaft, 21, in strictly radial antifriction bearings are provided in frame 24 placed in an opening in the base. The shaft is faced with rotating disk 23 with an edge stop for a hinged lever—double-arm lever 26. The cylindrical (axle) hinge, 19, is semi-encompassed by a helical compensating spring, 25, that orients the lever and the rotating ball, 27, relative to the diaphragm in the working (according to the principle of a variable-speed

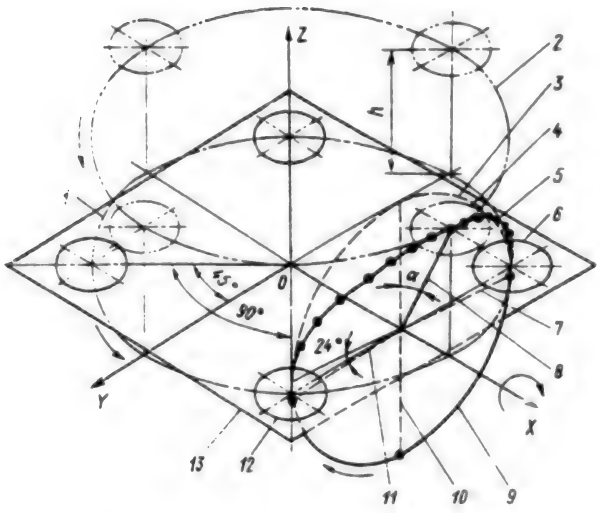

Figure 2. Axonometric Oblique-Angled Projection Drawing of Periodic Mutual-Contact Coupling and Foreshortened Trajectory of Drive's Driving Ball and Separator's Driven Diaphragm

differential with a rolling element) and no-load sections of the path described by the ball. The length of the arm to the ball's axle is set. The rotor drive itself comprises an electric motor, 30, a horizontal speed reducer, 31, with a reducing coupling, and pinion pair 32 and 22 of the gearing. The flanged bases of the two-sided ball sections ensure reliable securing and centering of the ball. The take-on shaft and drive form an angle of 45 or 90 degrees with the coordinates of the robot's base.

Graphic representations (fig 2) of the functional relationship between the driving ball - lever 8 (11, 7, 10) of the drive and the driven diaphragm, 13, of the separator clearly demonstrate the robot's specific features (one-way rotation, transportability, inertialess character—smooth pivoting with simultaneous elevating or lowering, mobility, equal and repeating periodicity—pivoting discreteness, constancy of behavior- -the algorithm for operating and for varying the angles of turn).

In the coordinate system used the abscissa (X axis) is in line with the axis of the take-on shaft, the ordinate (Z axis) [as published], of the separator's frame (diaphragm), and the Z axis (Y axis) [as published], of the extension (receiving) section of the cross (roller conveyer). At the initial instant the ball (lever 11, fig 2) places, via hole 12, the square diaphragm in a position whereby the diaphragm's diagonals are spaced at an angle of 45 degrees (angle between diagonals of 90 degrees) from horizontal axes X and Y. By the rotation of the take-on shaft, the ball is brought out of the state of rest. During the period that the lever turns by an angle of 204 degrees (position 7 in fig 2), it completes its working motion over a quite complex path in space—brachistochrone 5. At position 6 it is freed from the hole in the diaphragm, which is shifted from position to position, and it completes the prescribed path with a no-load motion (156 degrees) along arc 9 lying in an abstracted vertical plane, and it returns to the starting (initial) position and orients the diaphram relative to the next hole.

The ball rotates in a clockwise direction at uniform speed. With this, the following change simultaneously at each coordinated instant (the geometrical points on the trajectory): First, the following grow from zero to their maximum values: the height, h , to which the diaphragm is elevated (hole 4), the diaphragm's being rotated by the ball in the reverse direction; and the angle of deviation, α , of the ball (spring-operated lever 8 in fig 2) from the assumed arc, 3, of the flattened base circle and, corresponding to it, the nominally fixed vertical position (10 in fig 2) of the lever. The values of these same parameters drop from their maximum to zero in the second half of the complex motion sequence. The diaphragm's rate of smooth travel is equal or close to zero in both cases at the beginning and end of the working motion while the ball rotates by an angle of 24 degrees, because in these sections it is the horizontal component of the ball's linear rotational speed. Let us note that the error resulting from the small (five percent) difference between the length of the lever and the segment of its projection onto the vertical (planeness) was disregarded in establishing the real nature of the change and in geometrical plotting of the ball's additive trajectory.

The diaphragm turns by an angle of 90 degrees in each cycle (complete rotation of the ball). At any instant the holes lie in parallel and alternately changing abstract spatial planes having circular outlines, 1 and 2, projected onto a horizontal equidistant plane.

The specialized integrated-transport flexible systems (fig 3) include, in addition to functionally principal priority elements and motion converter robots, adapted and rapidly resettable roller conveyers furnished with individual and independent drives. Identifiable combined arrangements and designs completely satisfying the requirements of production are imparted to systems by the addition of some and the substraction of other coupled components. The multivariant character of the arrangements does not result in additional expenditures in this case.

All processes—motive and control functions—are performed automatically in a set sequence. The operating cycle can be continuous and intermittent.

The carrying (feeding, 3, and intermediate, 4) roller conveyers deliver a vertically positioned blank (part) to the robot and in per-unit collaboration gradually convey it to the rotating grooved rollers, 42 (cf. fig 1), which add an above-diaphragm section to the roller conveyer.

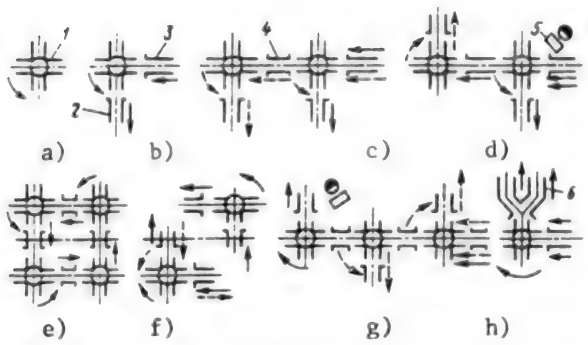

Figure 3. Some Implemented (a to d) and Standby (e to h) Integrated Robotized Systems

Key: 1—manipulator robot; 2, 3, 4—receiving, feeding and intermediate roller conveyers, respectively; 5—operation console; 6—receiving twin branched roller conveyer

The blank, 12, is conveyed by these same rollers between pairs of upper, 8, and lower, 4, guide rollers and above supporting plates, 37, to stop 2, and it actuates the electric limit switch—the robot's drive is put into operation. Rotating differential ball 27 of lever 26 raises diaphragm 28 (separator 5 and master cam 13) by 15 mm—the transverse supporting plates remove the blank from the grooved rollers and the limit switch. The ball forces the diaphragm, separator with the blank and the master cam to the extreme (limiting) upper position and lowers them to the extreme lower position and smoothly rotates them by a quarter-circle (a quadrant). With this, the master cam disengages from bearings 15 and engages with them after turning, and locks at set coordinates the separator and next hole of the diaphragm. The forced mechanical oscillations of the diaphragm are damped at the end of the ball's working motion, and the blank is placed on grooved rollers 39, which convey it from the separator to the receiving roller conveyer. The ball completes its no-load motion, and during this time the next blank, designed for transporting by "transfer" from roller conveyer to roller conveyer, arrives at stop 2. The pace and time cycle of the operation of all units of the system are coordinated and programmed. Serviceability deterioration and failures have not been observed.

The automated systems successively transport individual (one after the other) and specified—side-by-side and oriented in pairs—blanks in one direction (cf. fig 3b and e) or two directions (one-way and different-way; fig 3c, d and f to h) within the limits of local (fig 3a), differentiated (fig 3b to d and f to h) and circular—closed—(fig 3e) gripper working spaces. In a number of cases one robot changes the direction of the first blank but passes the next blank behind it to another robot (fig 3c and d), or the first two robots alternately turn "their" blanks and pass the next one to a third robot (fig 3g). Single and double (fig 3h) outlet roller conveyers are used.

Technical Data on Robot Systems

Number of orientation and transfer degrees of mobility of robot	6
Diameter of drive ball of robot drive, mm	50
Maximum angle of deviation, α , of lever from vertical, degrees	17
Working area of ball (lever), degrees:	
Limiting (maximum)Tc204	
Acceptable (minimum)	180
Axial working travel of lower semiaxle—amount of elevation (lowering) of separator, mm	90
Adjustable clearance (gap) between guide rollers, mm	40
Recordable smooth angle of turn of separator per rotation, degrees	90, 180
	270, 360
Time for separator to turn 90 degrees, s	5
Spacing of grooved drive rollers, mm	250
Rated power of drive electric motor, kW	2.4
Dimensions of robot (without drive), mm:	
Length (width)	1240
Height	2120
Maximum dimensions of blank (part), mm:	
Length (height)	1650
Width	1230
Transverse dimension of blank (blanks) or part) (thickness, depth of relief), not greater than, mm	35
Maximum weight of blank (part), kg	50
Time for complete robot cycle, s	9
Productivity of robot, pieces per hour	700

The broad-purpose systems are suitable for transport-and-transfer, orienting, exhibiting-and-turning (dynamic and static modeling) and fixing processes in cutting-and-preparing, process, thermal, assembling-and-welding and assembly, lubricating-and-blasting, washing-and-cleaning, painting and testing operations in the manufacture of parts made of various materials (metal, laminated and block plastics, wood—plywood, glass, cardboard, fiberboard, etc.) and on any scale at enterprises and corporations of the machine building complex.

Conclusions

The long-term use of robot and robot systems is confirming the profitability and promise, versatility (flexibility) and potential predominance of the field of their application and development. Working conditions have been improved significantly and operation safety is guaranteed. Some types of overhead conveyers and transport equipment are being replaced[1] and others are being made more efficient[2]. Blanks and parts are being protected reliably from unforeseen damage, breakage and possible flaws, their quality is being maintained and the materials consumption standard is not being lowered[3, 4]. Four workers have been freed.

Labor productivity has grown by a factor of 2.5. The generalized modernization coefficients and mobility indicators for transport equipment have been improved. The total annual saving is 78,000 rubles.

References

1. N.V. Potekushin and S.A. Svetlov, "Mechanized Line in Preparation Department," MASHINOSTROITEL, Nos 2-3, 1956, pp 29-31.

2. USSR Inventor's Certificate 1138362, MKI V 65 G 17/00, "Device for Suspending Items on a Hanger."

3. N.V. Potekushin and Yu.I. Shumilov, *Ekonomiya materialov i povysheniye kachestva izdeliy v kholodnoshtampovochnom proizvodste (Economizing on Materials and Improving the Quality of Products in Cold Forging Production)*, Moscow, Mashinostroyeniye, 1983, 89 pages.

4. N.V. Potekushin, "Mechanization of Cutting of Plate Material" in *Kholodnaya shtampovka, rubka, kalibrovka i volocheniye (Cold Forging, Slicing, Coining and Drawing)*, Moscow, VINITI, 1957, p 20.

UDC 658.52.011.56.012.315.02.89

Express Diagnosis of an Enterprise's Readiness To Create FMS

917F0077A Moscow MEKHANIZATSIYA I AVTOMATIZATSIYA PROIZVODSTVA in Russian No 10, Oct 90 pp 36-38

[Article by A.N. Kolosov, candidate of economic sciences, and Yu.G. Svirdyuk and A.G. Dibrov, engineers, under the "Economics and Organization of Production" rubric: "Express Diagnosis of an Enterprise's Readiness To Create FMS"]

[Text] The transition to new management methods increasing enterprises' independence in selecting the most efficient directions of automating manufacturing requires economically feasible solutions in all stages of substantiating, designing, and introducing new technology.

Under the current conditions at existing enterprises, there are often no obvious assessments of the need, possibility, or feasibility of developing automation in the form of flexible manufacturing systems [FMS]. Conducting a predesign analysis and technical-economic substantiation (with all the calculations) for even one version of creating an FMS is extremely laborious. The proposed express diagnosis method for determining an enterprise's readiness to create an FMS using computer technology based on the enterprise's subject area data base reduces the laboriousness of the calculations and permits a more purposeful selection of a version of developing an FMS even in the predesign stage.

The main purpose of express diagnosis is to make a well-founded decision regarding the feasibility of undertaking work to create FMS under specific industrial and technological conditions with a consolidated identification of its key parameters and an estimate of its anticipated effectiveness.

An idea of how ready an enterprise is for integrated FMS-based automation can be gained by estimating the need for and capability and feasibility of such automation in the given industry.

The need to create an FMS in an existing industry is substantiated by the difficulties that enterprises encounter during their operation and when determining changes that, thanks to the creation of an FMS, increase an existing industry's capability to function more efficiently.

The possibility of creating an FMS in an existing industry is assessed by analyzing the existing resources needed to design, introduce, and operate it. The analysis should reflect the status of the engineering and technological base, physical and financial resources, the scientific methodological base, and personnel resources under specific industrial conditions. The maximum amount of average yearly economic effect as the potential savings in the yearly adjusted costs of the industry's production under the conditions of the proposed version of an FMS as compared with the conditions of the existing production process is the criterion for the most feasible version of creating an FMS.

The proposed approach makes it possible to conduct an express analysis of an enterprise to obtain its generalized characteristics as well as the technical and economic indicators of the proposed versions of FMS with different automation levels in the absence of all the information required for more detailed calculations. The feasibility of creating an FMS of the required level is substantiated by modeling the technical and economic indicators of the design versions in comparison with the existing manufacturing process. The forecast assessments of the FMS are modeled by using a set of normative indicators, expert estimates, and existing data regarding operating FMS.

Seven levels and 12 sublevels of automating manufacturing systems based on the degree of increase in the number of functions performed automatically have been adopted to perform the technical and economic substantiation. Their characteristics are presented in Table 1.

Table 1

Automation Level Code	Characteristics of Manufacturing Systems' Automation Level	Automation Sublevel Code	Characteristics of Manufacturing Systems' Sublevel	Comment
1	Manufacturing systems with no devices for automatic control of machining (manufacturing equipped with manually controlled universal equipment)			Mechanized machine as per classification**
2	Manufacturing systems including devices for automatic control of the shaping process (manufacturing equipped with NC machine tools)	2.1	System of self-contained dedicated NC machine tools	Semiautomatic machine as per classification**
		2.2	System of self-contained NC machine tools with a tool magazine	
		2.3	System of self-contained NC machine tools of the machining center [OTs] and TOTs [expansion not given] NC types	
3	Manufacturing systems including devices to automatically feed (configure) blanks in the live zone (robot systems of machining centers with satellite-tables near machine tools, sections of NC machine tools and with AS [expansion not give], etc.	3.1	Robot systems based on dedicated NC machine tools	Automatic machines as per classification**
		3.2.	Robot systems based on machining center-type machine tools with an automatic satellite changer	
		3.3.	Robot system with an automatic warehousing and transport system with autonomous control	
4	Manufacturing systems with automatic realignment to manufacture established products (flexible manufacturing modules, sections of flexible manufacturing modules with automatic alignment systems)	4.1	Flexible manufacturing modules connected via automatic transport to a computer-controlled machining tool group	First-level automation of FMS as per*
		4.2	Flexible manufacturing module + automatic alignment system + automatic FMS control system	
5	Manufacturing systems with automatic realignment to manufacture established products (sections and shops including flexible manufacturing modules with a control computer system)	5.1	Flexible manufacturing modules equipped with equipment to monitor the presence and status of tooling and to realign tooling + an automatic alignment system + an automatic FMS control system	Second-level automation of FMS as per*
		5.2	Flexible manufacturing modules equipped with equipment to monitor the quality of machining and loading of attachments + an automatic alignment system + an automatic FMS control system	
6	Manufacturing systems with automatic realignment to manufacture new products (FMS including an ASTPP [expansion not given], automatic control system, etc.)	6.1	Flexible manufacturing modules equipped with equipment to change tooling sets and with equipment to monitor attachments and their fine adjustment	Third-level automation of FMS as per*

*GOST 26962-86; **Metodicheskiye ukazaniya po otsenke stepeni i urovnya avtomatizatsii proizvodstva (Methodological Directives on Assessing the Degree and Level of Production Automation), decreed by the USSR State Committee on Science and Technology [GKNT] on 7 Aug 1985, No. 425.

Levels 4, 5, and 6 of FMS-based automation have been adopted in GOST 26962-85.[1] The automation levels of the existing manufacturing process (base variation) is identified along with proposed versions of integrated automation of manufacturing based on FMS.

The distinctive features of the predesign stage made it necessary to use a calculation procedure that is the opposite of the conventional determination of economic effectiveness, namely, calculation based on economic effect indicators, to determine the required technical and technological parameters of the versions of an FMS.

The method focuses mainly on estimating (without any design developments) the anticipated changes in the technical and economic indicators of the manufacturing process given one version of an FMS or another. This estimate is made by introducing into the calculations systems of coefficients reflecting the mean ratio of the values of the technical and economic indicators

Table 2.

Базовый вариант уровня и подуровня автоматизации (1)			Проектный вариант уровня и подуровня автоматизации (2)								
			1	2				3	4	5	6
				2.1		2.2	2.3				
				2.1.1*	2.1.2*						
	1		1	$0.76^{0.09}$	$0.67^{0.13}$	$0.56^{0.08}$	$0.38^{0.10}$	$0.82^{0.09}$	$0.79^{0.08}$	$0.76^{0.08}$	$0.73^{0.10}$
2	2.1	2.1.1		1	$0.88^{0.12}$	$0.74^{0.16}$	$0.50^{0.15}$	$0.75^{0.10}$	$0.75^{0.12}$	$0.47^{0.13}$	$0.65^{0.10}$
		2.1.2			1	$0.94^{0.15}$	$0.57^{0.16}$			$0.54^{0.12}$	
	2.2					1	$0.68^{0.12}$			$0.64^{0.12}$	
	2.3						1			$0.94^{0.06}$	
3								1	$0.61^{0.16}$	$0.50^{0.09}$	$0.50^{0.11}$
4									1	$0.62^{0.08}$	$0.58^{0.10}$
5										1	$0.63^{0.12}$
6											1

* Станки с преднабором и цифровой индикацией (3)
** Станки с ЧПУ (4)

Key: 1. Base Version: Automation Levels and Sublevels 2. Design Version: Automation Levels and Sublevels 3. *Machine tools with preview and digital display 4. sup**NC machine tools

observed in industries with different levels of automation, including automation based on FMS.

Provided a sufficient source base reflecting the experience accumulated during the operation of existing FMS is present and provided it is constantly expanded with correct grouping of the significant properties of the manufacturing system, such coefficients may predict the anticipated values with a precision that is adequate for preliminary estimates. Calculations made by the authors, including calculations considering published data,[2] show, for example, that when different versions of replacing machining equipment are used, the time required to machine a workpiece belonging to a specific class changes in the proportions presented in Table 2 regardless of the workpiece's overall dimensions.

The full set of similar coefficients includes the following:

—the coefficient of the change in machine tool capacity in the industry K_{cap} as the ratio of the time required to machine one workpiece in the design version t_{w2} to the time required in the base version t_{w1};

—the coefficient of the increase in the cost of a unit of machining equipment K_0 as the ratio of the yearly adjusted costs to acquire, install, and amortize equipment in accordance with the design version C_{02} to the time required in the case of the base version C_{01};

—the coefficient of the change in the number of persons servicing equipment K_0 as the ratio of the specific norms for numbers of personnel (calculated for one machine tool) in accordance with the design version $H_{No.2}$ to the number required in the case of the base version $H_{No.1}$;

—the coefficient of the change in wages and social costs per worker K_{wg} as the ratio of the given amounts in the design and base versions ($C_{No.2}$ and $C_{No.1}$, respectively);

—the coefficient of the use of hourly equipment operating costs K_{op} as the ratio of the given amounts in the case of the design and base versions (C_{op2} and C_{op1}, respectively);

—the coefficient of the change in the duration of the production cycle entailed in machining one product (K_{cyc} as the ratio of the average duration of a cycle in accordance with the design and base versions (T_{cyc2} and T_{cyc1}, respectively);

—the coefficient of the change in costs for the technological preparation of production K_{tp} as the ratio of the given amounts calculated for a single operation in accordance with the design (C_{tp2}) and base (C_{tp1}) versions;

—the coefficient of concentration K_{con} by types of machining as the ratio of the number of operations in the design (D_2) and base (D_1) versions.

The yearly economic effect derived from introducing a design FMS with any automation level (the subscript 2) in place of the base version (the subscript 1) is determined by the difference in the adjusted costs based on the following formula:

$$E = C_{01}R_1(B_2/B_1-K_0K_{cap}K_{sh2}) + H_{No.}R_1 \times C_{No.1}F_{sh}K_{sh1}(B_2/B_1-K_{wg}K_{cap}K_{No.}) + C_{op1}F \times K_{sh1}R_1(B_2/B_1 - K_{cap}K_{op}) + C_wK_{inc}T_{cyc1}E_n(B_2/B_1-K_{cyc}) + C_{tp1}D_1(1-K_{tp}K_{con})-E_nC_{pre} + (B_2/B_1-1)C_wD_{wor}H_{pro}/100, \quad (1)$$

where B_2/B_1 is the index of the production volume in the design and base versions, K_{sh1}/K_{sh2} is the ratio of the machine shift coefficients in the base and design versions, R_1 is the amount of equipment in the base version that machines a yearly program's worth of workpieces (in pieces), F_{sh} is the per-shift actual yearly fund of workers' time (in hours), C_w is the cost of the average daily output of workpieces in the base version (in rubles), F_{eq} is the per-shift actual fund of equipment operating time (annual) (in hours), K_{inc} is the coefficient of the cost increase, E_n is the normative coefficient of the economic effectiveness of capital investments, D_{wor} is the number of worker-days per year, H_{pro} is the profit norm (%), and C_{pre} represents the preproduction costs (in rubles).

The effect estimate in accordance with formula (1) is performed for different versions of FMS-base automation of production. These versions are formulated by combining an automation level (Table 1) and selected automation objects, i.e., technological-design groupings of workpieces. The following are required for the calculations: source information (the base version indicators with the subscript 1) and a set of reference information on standards relative to the change in indicators (see Table 2). The characteristics of the existing manufacturing process are confined to the indicators C_{01}, $H_{No.1}$, $C_{No.1}$, C_{op1}, T_{cyc1}, C_{tp}, D_1, R_1, C_w, K_{inc}, D_{wor}, and H_{pro}, the values of which are established on the basis of the enterprise's accounting data and on the basis of workpiece sketches and technological documentation. A number of indicators ($H_{No.1}$ and C_{tp1}) are initially formulated on the basis of groupings of workpieces and equipment used.

As the automation versions are formulated, the indicators are consolidated, and their average weighted values are taken for the calculations.

Table 3

Level and Sublevel of FMS-Based Manufacturing	Average Yearly Economic Effect From Creating FMS Based on Machining Workpieces From Classification Groups* (in thousands of rubles)								Total Economic Effect (in thousands of rubles)
	1D	2D	3D	4D	1V	2V	3V	4V	
2.3	12.4	16.3	25.3	28.2	13.6	14.2	17.2	27.4	154.6
3**	18.2	24.2	12.2	19.1	24.1	25.9	24.5	12.2	160.4
4	9.1	2.5	-0.7	8.2	16.2	7.8	10.5	2.3	55.9
5	-2.5	-10.5	-8.6	3.1	2.5	-7.5	2.1	-10.5	-31.9
6	-15.4	-28.2	-16.2	-5.5	-2.5	-20.5	-3.5	-31.5	-125.3

*1D-4D and 1V-4V, type size groupings of body-of-revolution-type workpieces (disks and shafts); **Most efficient level of FMS.

For subsequent grouping, the workpieces are classified on the basis of the following features: the workpiece's structural type (bodies of revolution, base members, etc.), size characteristics, and complexity class.

The automation object is formulated by selecting and combining workpiece groupings with an allowance for preference rules. The type sizes of equipment needed for each version of grouping workpieces are determined along with their related costs (C_{01} and C_{op1}).

The ultimate purpose of the calculations based on formula (1) is to find that design version that would provide the maximum economic effect when compared with the base version.

The sequence of modeling the transition to the next level of automation consists of the following:

—from the sample of the subset of workpieces and operations that are slated for machining, make a switch to progressive equipment in accordance with the preference rules adopted;

—calculate the design machine tool capacity in the modeled version by correcting the base machine tool capacity with respect to machining the j-th workpiece in the k-th group on basis of the i-th equipment group:

$$t_{wijk2} + t_{wijk1}K_{cap} \quad (2)$$

—calculate the indicators of the version being modeled in accordance with formula (2);

—determine the yearly economic effect derived from using the modeled version of progressive equipment;

—proceed to the next workpiece subset, etc.

Operations related to formulating versions of automation objects, calculating the indicators of base and design versions, inputting reference information on standards, and revising versions are performed automatically by using a personal computer in the MS DOS operating environment. Table 3 presents a fragment of the result of the express diagnosis performed at the Voroshilovgrad Machinery Plant imeni A.Ya. Paarkhomenko. In addition to purely economic estimates of the versions, the process of making a diagnosis requiring up to 40 worker-days over the course of a month results in a whole series of technical and organizational parameters of prospective versions: the type size and automation level of equipment, its quantity and degree of loading, size of the work force, technological and design characteristics of workpieces, duration of their machining cycle, and other parameters that then serve as the basis for developing

that proposal for creating FMS that guarantees an increase in the economic effectiveness of the production process.

Footnotes

1. GOST 26962-86, Sistemy proizvodstvennyye gibkiye. Moduli proizvodstvennyye gibkiye (Flexible Manufacturing Systems. Flexible Manufacturing Modules), Moscow, Izd-vo standartov, 1986.

2. V.L. Kublanov, I.A. Makovetskaya, A.P. Nazarenko, et al., Ekonomicheskoye obosnovaniye oblasti primenieniya metallorezhushchikh stankov s programmnym upravleniyem (Economic Substantiation of the Area of Application of Metal-Cutting Machine Tools With Program Control), Moscow, Mashinostroyeniye, 1987.

Bibliography

A.K. Martynov, Gibkiye proizvodstvennyye sistemy mekhanicheskoy obrabotki v edinichnom i melkoseriynom proizvodstve detaley tochnoy mekhaniki (Flexible Manufacturing Systems for Machining in Single-Unit and Small-Series Production of Precision Mechanics Components), Izd-vo Tomsk un-ta, Tomsk, 1988, 308 pages.

UDC 621.74:621.313:658.382:538.4

Using MHD Devices To Mechanize and Automate Chemistry, Metallurgy, and Other Sectors

917F0068A Moscow MEKHANIZATSIYA I AVTOMATIZATSIYA PROIZVODSTVA in Russian No 7, Jul 90 pp 1-3

[Article by V.M. Foliforov and V.S. Gorovits, candidates of technical sciences, under the "Automating Production Processes" rubric: "Using MHD Devices To Mechanize and Automate Chemistry, Metallurgy, and Other Sectors"]

[Text] One of the most complicated problems arising during the development of systems to mechanize and automate metallurgical processes is that of creating devices to control the movement of melts and to monitor this movement. The main difficulties are related to the fact that the melts are highly aggressive and have high temperatures. Soviet and foreign researchers have created a number of magnetohydrodynamic [MHD] production devices using a magnetic field to effect actions on melts without direct contact.

MHD methods and devices may be used in metallurgy and foundry work, in the power generation and chemical industries, at nuclear power plants, in space technology, and at thermonuclear synthesis installations—everywhere where conductive liquids are used for some production-related purpose.[1]

The principle of the operation of MHD devices may be reduced to the following:

1. If a current is passed through conductive liquid located in a magnetic field, a force field will arise in the liquid that causes it to move.

2. If the conductive liquid moves in the magnetic field, an electrical field will arise in the liquid.

The operation of MHD devices exerting a force effect on a melt is based on the first principle, while electromagnetic flowmeters and MHD generators operate in accordance with the second principle. Both principles are often used in engineering MHD devices.

It follows from what has been said that the latest progress in electrical machinery building, metallurgy, heat engineering, and the technology of refractories and electrical insulation materials is used in creating MHD devices.

We will briefly examine the main types of MHD devices that are used in industry.

The best-known example of an MHD device in which a force effect is exerted on a melt are electromagnetic pumps, which are widely used as actuating mechanisms in systems to transport and meter liquid metals.

Several main types of electromagnetic pumps exist: induction and conduction.

The operation of an electromagnetic pump may be explained by way of the example of a conduction pump consisting of a rectangular channel to which electrodes have been fastened. The channel itself is located in the magnet's gap. When current passes through the melt between the electrodes as a result of its interaction with the magnetic field, a force is created that moves the melt in the required direction. Pumps of this type have a comparatively high efficiency and good weight and size characteristics and can operate under rigid thermal conditions; however, they require special power sources and are complex and expensive. They are therefore used in places where there is a current source (for example, in combination with thermoelements) where high radiation resistance requirements are imposed or else where the electric conduction of the melt is low.

Combinations of a alternating-current conduction pump and transformer are somewhat more convenient to operate. The power source requirements are eased.

Induction pumps are an interesting and very promising type of electromagnetic pump. By using a special system of conductors located in the magnetic system, these pumps create a traveling magnetic field in the melt located in the channel (plane, round, etc.) that entrains the melt and creates electric forces in it. These pumps are used to transport alkali metals, aluminum, mercury, lead, tin, their alloys, and other metals. They have found

application in nuclear power and different production installations. Electromagnetic induction pumps develop a pressure up to 6×10^6 Pa and feed metal in a flow rate up to 3,000 m^3/h at a temperature up to 600°C, are exceptionally reliable, and have smooth control characteristics. That version of an induction pump with an open channel has received the name electric trough. It is a trough made of refractory. It is open from the top, and a magnetic system is mounted on one of its sides. This type of device is easily installed in metallurgical melting furnaces and permits a sharp acceleration in the preparation of alloys in furnaces, metal refining, variation of a composition, automation and mechanization of the processes of casting, and metered pouring of metals.

Common advantages of all electromagnetic pumps and all the devices examined from here onward is that their flow path is leak-tight, they have no moving parts, their operating characteristics are directly controlled by changing their electrical values (current, voltage) and thus lend themselves to smooth remote control, and they make it possible to create simple and reliable automatic production process control systems.

Next, we will examine one class of production MHD devices, i.e., mixers. Liquid melts and solutions may be mixed for the following purposes: accelerate the mass exchange processes at the interfaces of solid and liquid phases, even out the concentration of substances in the volume of a melt, even out the temperature distribution, change the gradients of the concentration of substances in a melt, control the course of electromagnetic reactions by cleaning the electrodes' surfaces, and accelerate the processes of purifying melts.

In conventional metallurgical devices these tasks are performed by using mechanical devices that possess a number of shortcomings from a technological standpoint: low stability of the material in the melt, high heat losses, appearance of foreign inclusions and impurities in the metal, no leak tightness of the processes, and complexity of controlling the mode of the effect.

MHD mixers, which can be used to mix an entire melt and to feed a melt into a reagent in drop form, do not have these defects.

The designs of mixing MHD devices may differ sharply: They may be conduction devices or induction traveling field devices. They may use currents already existing in the production processes, for example, during electrolysis.

Electromagnetic mixers make it possible to accomplish the following:

increase the speed of chemical refining of mercury by a factor of 20 and increase the speed of floating-zone refining of semiconductor materials by a factor of 3 to 5, increase mixers' capacity with respect to preparing aluminum alloys by about 20%, increase the production speed and homogeneity of optical glasses, reduce losses of mercury during the process of producing chlorine and caustic soda by the method of electrolysis on a mercury cathode, use electromagnetic mixing to produce alloys with an unusual content of some component, and improve the structure of castings produced by the continuous method and by casting in a chill mold.

The mixers may be located outside the tank holding the melt or inside it (immersible).

Magnetohydrodynamic methods not only make it possible to mechanize and improve conventional production processes, but they also create fundamentally new production capabilities related to the selectivity of an electromagnetic effect on heterogeneous systems whose components possess different properties (for example, slag-metal systems, mixtures of different metals, suspensions, etc.).

Also interesting are MHD devices in which electric and magnetic fields are used to create a static force field that is analogous to a gravity field in many respects. Using such forces makes it possible to control the effective density of liquid and act selectively upon particles in heterogeneous systems.

These devices may be used in separating mixtures, producing alloys made of nonmixing substances (of the "frozen emulsion" type), and controlling the reaction rate in heterogeneous systems. These devices are currently in the R&D stage.

MHD oscillators intended to create waves or streams of solder to wash prepared printed circuit board surfaces as they move continuously over the solder melt have enjoyed wide-scale use in the technology of manufacturing printed circuit boards and units for electronic equipment. These devices make it possible to control the technological parameters of the soldering process within broad bounds and provide high-quality soldered joints. The main advantages of MHD oscillators are as follows: there are no moving parts, which reduces contamination of the solder; the amount of solder in a unit's bath may be reduced by a factor of 2-3; they have small overall dimensions; only a short warming time is required to prepare for operation; and most of the power consumed by the oscillator goes to heat the solder, which reduces the load of the heaters and increases their reliability. Devices with a wave width up to 420 mm currently exist.

In a number of engineering applications using liquid metals devices are required that are capable of functioning as gates, slide valves, and stops with exceptional simplicity, high reliability, and selectivity of their effect. MHD valves and stops belong to this class of device. Electromagnetic pumps in which the force is directed counter to the flow of the melt or special valves in which a permanent magnetic field that may change the pressure

loss of the flow path by a factor of 10 may be used as stops. These devices may be useful in nuclear power generation, metallurgy, etc.

One version of an MHD valve is a device to suppress flows and reduce pulsations during the process of growing monocrystals of semiconductor materials, for example, silicon. Using such devices makes it possible to produce monocrystals with a low oxygen content and highly uniform distribution of impurities in the crystal.

MHD stops (valves) may be used to solve the problem of hot application of anticorrosion metal coatings (aluminum, aluminozinc alloys) on long steel products and intermediate products (an angle, channel iron, circle of pipe, etc.) by using through baths. MHD stops are selective: They prevent the melt from flowing out while at the same time do not interfere with the passage of solid objects. A through bath, unlike dipping baths, have smaller overall dimensions, use less metal (by a factor of 5-10), and cost less. A through bath has holes located below the level of molten metal through which the products being treated pass. The melt is kept from leaking out of the bath's windows by MHD valves. In addition, MHD valves heat the metal in the windows. The through holes in the windows are made of a material that is stable in the melt. The devices developed may be used to apply aluminum coatings to angles with flange dimensions up to 160 mm, pipe up to 180 mm in diameter, and sheet stock up to 700 mm wide and 0.5 to 2 mm thick. Not only do these devices make it possible to reduce the baths' consumption of metals and cost, but they also have the following advantages: the length of treatable products is unlimited; the process of applying coatings is fully mechanized; the unit is highly reliable, and its mean time between repairs is longer; the coating quality is higher on account of a reduction of the amount of iron in the melt and a reduction in the underlayer of intermetallides (by almost a factor of 10) thanks to a reduction in the product's path in the melt; the coating's quality (thickness and make-up) can be controlled; and they afford the capability of bilaterally aluminizing pipes.

The units now existing in the metallurgy industry were developed over a long period of time and form a harmonious, efficient system despite the fact that they are designed and constructed on the basis of obsolete principles. For this reason, using MHD devices in individual sections, even the "narrowest" sections, can possibly fail to produce the anticipated effect. What is feasible is the integrated introduction of MHD devices with a unified component base affording the capability of mechanizing and automating the entire metallurgical conversion process. One example of such introduction is the system of MHD devices to produce high-purity mercury. A series of pumps for mercury (with a head from 13 kPa to 3.5 MPa and a capacity from 2 to 60 t/h), chemical refining devices, devices for metered pouring (from 5 to 34.5 kg) with a precision up to 0.05%, and devices for vacuum distillation and electrolytic refining of mercury was developed on a unified component base. These devices helped create fully automated and leak-tight, ecologically clean production of high-purity (all the way up to 99.999999%) mercury. Manual labor was completely eliminated all the way from the production of ferrous metallurgical mercury to the output of finished product.

The mercury produced in this production process, which contains a low content of residual gases, served as the basis for organizing the manufacture of a new product—getter-mercury fillers (batchers) for luminescence and gas discharge tubes. These fillers are an intermetallic compound of titanium and mercury that, when heated, decompose. In so doing, they release mercury while the titanium absorbs the residual gases at the same temperature. Getter-mercury batchers are manufactured in the form of tables, powder, or strips with a preapplied quantity of titanium mercuride. Using them simplifies the technology of manufacturing tubes, solves the problems of destroying depleted tubes, and increases the light yield and useful life of luminescent tubes (up to 20,000 hours). An original technology for producing this substance that ensures its high quality (high mercury content and infinitesimal residual gas content) has been developed along with high-productivity equipment producing source titanium powder without preliminary degassing.

In industry, when systems to automate production processes are developed, precise measurement of the flow rate and amount of liquid and its metering becomes necessary. Solving this problem, particularly for melts, is possible by using electromagnetic flowmeters in which the electric signal arising in a melt as it moves in a magnetic field is used to determine the melt's velocity or flow rate. The best known are the so-called conduction flowmeters in which the voltage arising in a channel as liquid moves is directly measured. To increase the precision of measuring the flow rate, the latest electromagnetic conduction flowmeters intended to measure the flow rate of liquid metals or melts with ion conduction (water and solutions) are based on the measurement principle according to which the ratio of the signal associated with the velocity to the auxiliary signal (which includes an allowance for the parameters of the working medium, power source, etc.) is used instead of the velocity itself. This provides the following advantages:

—increases the precision of measuring the flow rate over a broad temperature range by eliminating the instability of the sensor's magnetic field and zero drift;

—affords the capability of using a lighter-weight magnetic system;

—affords the capability of calculated calibration without any individual profuse calibration on metrologic stands.

Such flowmeters may be used to measure the flow rates of liquid metal coolants in the range from 0.2 to 50 l/s and at a temperature up to 1,000°C with a precision of flow rate measurement up to 1 to 1.5%. Installing a microprocessor makes it possible to measure the amount of liquid based on a specified program and permits

automatic diagnosis of functional nodes, zero adjustment, and calibration of the instrument.

In some cases, using contacts to extract signals causes specific problems related mainly to the stability of the materials in the melt. A series of noncontact flowmeter-batchers with a special system to read the velocity signal and the auxiliary reference signal have been developed to solve these problems. The flow rate is determined on the basis of the ratio of these signals. This flowmeter differs from those examined previously in that it provides the following: its readings are independent of the degree of wetting of walls with the melt, which permits its operation when wetting is poor and even when it is absent; the readings are independent of the melt's electric conduction and the change in the sensor's magnetic field, which provides precision over a broad temperature range; it permits calculated calibration; and it suppresses "zero" drift, which increases the stability and reproducibility of the results.

Such flowmeters make it possible to measure a flow rate in the range from 0.001 to 5 l/s with an error of 1 to 4%.

The electrification correlation flowmeter-batcher in which the time required for an electrified liquid flow to pass through two sections in a pipeline offers interesting possibilities for measuring liquid hydrocarbons and suspensions based on them in flows. Electrodes receiving the charge pulses arising during the turbulent motion of liquid along a pipeline are mounted in these sections. These signals are processed by a microprocessor, and their correlation is used as the basis for determining the flow rate or amount of liquid.

All flowmeters have digital readout and normalized current leads.

Most MHD devices are developed on the basis of individual designs and tied to a specific production device or process, which ensures their highly efficient use.

Footnote

1. The information presented here is based on the results of developments at the Magnetohydrodynamics Special Design Office of the Physics Institute of the LaSSR Academy of Sciences. The authors thank comrades E.A. Isidorova, B.L. Birgera, I.P. Kvasnevskiy, G.Kh. Kirkhshteyn, and G.G. Gurevich for providing materials regarding their work.

Magnetic Field Instead of a Reducing Gear

917F0101A Moscow IZOBRETATEL I RATSIONALIZATOR in Russian No 8, Aug 90 pp 12-13

[Article by V. Volodin; first paragraph is boldface IZOBRETATEL I RATSIONALIZATOR subheadline]

[Text] Only a few people know that a magnetic field may replace a conventional pinion in a reducing gear. In any case, it is not mentioned in the higher educational institution-level course in machinery components dealing with mechanisms with magnetic coupling. Nevertheless, gears without any mesh, with lead screws that "flail" freely in nuts, and with clutches in which the driving and driven halves do not make any contact with each other at all operate in machine tools and mechanisms (albeit in only a few so far).

Just what kind of mechanisms are these?

We will take the reducing gear as an example. Outwardly it is entirely ordinary. On one side of the casing there is a drive shaft connected to an electric motor; on the other side there is a driven shaft. But if the reducing gear's casing were transparent, the fact that the gears, i.e., the traditional filling of reducing gears, make no contact with one another would become immediately clear. And the profile of the teeth of these strange gears are not at all evolvent but are instead rectangular, as are the tooth spaces between them. The rotation of the drive shaft is nevertheless transmitted to the driven shaft through the cascade of noncontacting gears. And according to the very same law as in the case of a conventional gearing! The difference between the rotation speeds of the driven and drive wheels equals the difference between the numbers of teeth on the driven wheel and on the drive wheel.

The point is that the teeth of the drive wheel are individual permanent magnets. When the system is at rest, only a radially directed force acts between the magnet-tooth of the drive wheel and the opposing tooth of the driven wheel. To put it simply, the drive wheel, as if put to a magnet, attracts the driven wheel to it self. As it rotates, the drive wheel tooth tries to move away from the driven wheel, but it cannot break away because it is connected with it by magnetic forces. So it pulls the driven wheel along with it and thus turns it. As the rotation proceeds, the teeth move away from one another, the magnetic attraction between them weakens, and at some point it is as if the drive wheel loses the drive wheel (this would be the case if each wheel had only one tooth). But there are many teeth, and when one pair moves out of the magnetic "engagement", the next tooth moves into it. The driven wheel thus rotates continuously while the drive wheel rotates. In a word, it is just as in a conventional tooth pair. The more teeth there are on a drive wheel versus on the driven wheel, the higher the gear ratio and the faster the driven wheel rotates.

High rotation speeds may thus be transmitted with a rather high power transmission, for example, up to 20 kW at a speed of 30,000 rpm.

"And is this all necessary?" asks the reader justifiably. Indeed a conventional toothed reducing gear can have the same technical characteristics. But a magnetic reducing gear is noiseless, and its wheels do not wear out for all practical purposes. Since there is no contact between them, there is no friction. This means that no lubricant is necessary. No precise or complex evolvent

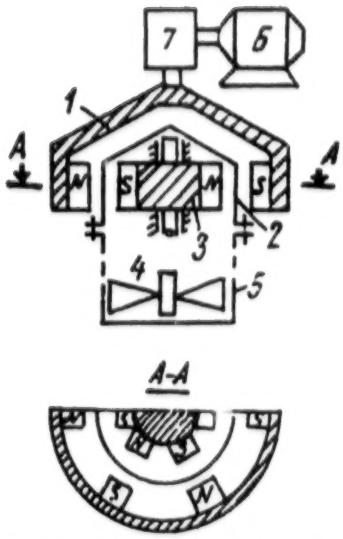

Figure 1. Diagram of the Drive of the Commercial Reducing Gear Mixer

Key: 1. driving half-coupling; 2. closure head (made of nonmagnetic metal); 3. driven half-coupling; 4. mixer plates secured to the shaft of the driven half-coupling; 5. reactor vessel. The half-couplings are separated from one another by a uniform air gap in which a fixed screen made of nonmagnetic material (the reactor vessel's closure head) is located. Permanent magnets with alternating polarity are located on the working surfaces of the half-couplings. As the driving half-coupling is rotated by an electric motor (6) through a conventional reducing gear (7), the magnets located on its inner surface are shifted relative to the magnets located on the driven half-coupling. Tangentially directed magnetic forces arise that entrain the driven coupling in a rotation that is in sync with that of the driving half-coupling. It is recommended that the screening closure head around which the driving half-coupling rotates be made of stainless steel or titanium.

profile is necessary. No careful machining of the gears, hardening, grinding, or cementing is necessary. If one of the wheels in such a mechanism locks suddenly, not one tooth will break. The drive wheel simple rotates under the motionless driven wheel.

But all these advantages pale next to the main one. A blind partition may be installed between the drive and driven wheels, even fingers' thick, and the driven wheel will nevertheless turn. The only condition is that the partition must be made of a nonmagnetic material. This advantage gives mechanisms with magnetic coupling great possibilities.

How, for example, can rotation be transmitted in a chamber with an ultrahigh vacuum? Should a drive shaft be passed into the chamber through a reliable seal in the wall? After some time, however, instruments will detect that there is no longer an ultrahigh vacuum in the chamber. Perhaps the reducing gear and electric motor can be mounted directly in the chamber, and the site where the electric drives pass through the chamber wall can be sealed completely reliably, for example, by filling the opening with epoxy resin. There will be no "leakages" in the vacuum. After a time, however, hydrocarbons, sulfur, and other impurities will appear in the pure space of the chamber, where molecules of oxygen, nitrogen, and carbon dioxide literally chase after one another in all the spaciousness. From where? From the working electric motor.

A mechanism with magnetic coupling solves the problem simply. The drive shaft and electric motor are mounted outside the chamber, whereas the driven shaft is inside it without any openings in the wall.

Imagine a shaft rotating on bearings without balls and rollers that are held in the center of the ring by magnetic forces. In such a bearing a shaft may make up to hundreds of thousands of rotations per minute. Only the friction of the shaft against the air interferes. If the shaft is turning in an ultrahigh vacuum, it will turn in unison with the bearing—if not with a permanent motor, at least with one lasting for many days. This shaft can only be turned in an ultrahigh vacuum by using a magnetic mechanism. The practical value of such a mechanism is hard to overestimate. In a "magnetic" centrifuge, for example, it is possible to generate enormous centrifugal forces, which opens up unique possibilities. It is possible, for example, to produce ultradense materials, use new diffusion processes, accumulate colossal mechanical energy in flywheels, and test all possible components for strength.

And magnetic mechanisms can transmit more than rotary motion. For example, they can be used when some plate has to be ground from metal that is ultrasensitive to oxygen. A small machine tool can be built in a vacuum chamber. A spindle with an abrasive stone can be turned by a magnetic reducing gear while the table holding the workpiece is moved to and fro by a magnetic toothed rack with a gear located and rotating outside the chamber.

Leningrad scholars have developed several dozens of mechanisms with magnetic coupling. It may be said that they may be used for all occasions—even in those cases where it would seem that nothing like them would ever be used. A magnetic reducing gear has, for example, been mounted in a mixer operating under a pressure of 100 atmospheres. Previously, 25 kW of the power required to turn the mixer's shaft was expended just to overcome the friction in "ultradense" packings. After a magnetic reducing gear was installed, the power losses were reduced to 1 kW.

But the more transmission mechanisms are located in a sealed chamber itself, the more difficult it becomes to maintain a specified atmospheric purity in that chamber.

At the Leningrad Forestry Engineering Academy imeni S.M. Kirov, researchers creating a number of chemical reactors used a conventional toothed reducing gear;

however, they mounted it outside the reducing gear's hermetically sealed casing. A magnetic coupling transmits the rotation from it to the mixer shaft, which is located in the hermetically sealed space. Like an "umbrella," the drive half-coupling rotates over a closure head made of nonmagnetic material, while the driven half-coupling is mounted under the closure head on the mixer shaft. Six permanent magnets that are evenly spaced along the perimeter of the drive half-coupling and the same number on the driven half-coupling transmit the torque with a rather high efficiency. For example, the losses (the currents of the rotating multipole system of permanent magnets heat the reactor vessel, which serves as a screen) do not exceed 1% to 2% of the transmitted energy.

Leningrad specialists developed magnetic couplings (magnets in the form of plates 25 x 12 x 116 mm) that turn mixers in commercial chemical reactors with capacities up to 6 cubic meters!

END OF FICHE DATE FILMED

5 April 1991